Check for updates

Possible Cross-Reactivity of Feline and White-Tailed Deer Antibodies against the SARS-CoV-2 Receptor Binding Domain

Trevor J. Hancock,[a] Peyton Hickman,[a] Niloo Kazerooni,[b] Melissa Kennedy,[b] [ID] Stephen A. Kania,[b] Michelle Dennis,[b] Nicole Szafranski,[b] Richard Gerhold,[b] Chunlei Su,[a] Tom Masi,[c] Stephen Smith,[d] [ID] Tim E. Sparer[a]

[a]Department of Microbiology, University of Tennessee, Knoxville, Tennessee, USA
[b]Department of Biomedical and Diagnostic Sciences, University of Tennessee, Knoxville, Tennessee, USA
[c]Graduate School of Medicine, University of Tennessee Medical Center, Knoxville, Tennessee, USA
[d]MEDIC Regional Blood Center, Knoxville, Tennessee, USA

ABSTRACT In late 2019, a novel coronavirus began circulating within humans in central China. It was designated SARS-CoV-2 because of its genetic similarities to the 2003 SARS coronavirus (SARS-CoV). Now that SARS-CoV-2 has spread worldwide, there is a risk of it establishing new animal reservoirs and recombination with native circulating coronaviruses. To screen local animal populations in the United States for exposure to SARS-like coronaviruses, we developed a serological assay using the receptor binding domain (RBD) from SARS-CoV-2. SARS-CoV-2's RBD is antigenically distinct from common human and animal coronaviruses, allowing us to identify animals previously infected with SARS-CoV or SARS-CoV-2. Using an indirect enzyme-linked immunosorbent assay (ELISA) for SARS-CoV-2's RBD, we screened serum from wild and domestic animals for the presence of antibodies against SARS-CoV-2's RBD. Surprisingly prepandemic feline serum samples submitted to the University of Tennessee Veterinary Hospital were ~50% positive for anti-SARS RBD antibodies. Some of these samples were serologically negative for feline coronavirus (FCoV), raising the question of the etiological agent generating anti-SARS-CoV-2 RBD cross-reactivity. We also identified several white-tailed deer from South Carolina with anti-SARS-CoV-2 antibodies. These results are intriguing, as cross-reactive antibodies toward SARS-CoV-2 RBD have not been reported to date. The etiological agent responsible for seropositivity was not readily apparent, but finding seropositive cats prior to the current SARS-CoV-2 pandemic highlights our lack of information about circulating coronaviruses in other species.

IMPORTANCE We report cross-reactive antibodies from prepandemic cats and postpandemic South Carolina white-tailed deer that are specific for that SARS-CoV RBD. There are several potential explanations for this cross-reactivity, each with important implications to coronavirus disease surveillance. Perhaps the most intriguing possibility is the existence and transmission of an etiological agent (such as another coronavirus) with similarity to SARS-CoV-2's RBD region. However, we lack conclusive evidence of prepandemic transmission of a SARS-like virus. Our findings provide impetus for the adoption of a One Health Initiative focusing on infectious disease surveillance of multiple animal species to predict the next zoonotic transmission to humans and future pandemics.

KEYWORDS ELISA, RBD, SARS-CoV-2, antibodies, bovine, canine, coronavirus, cross-reactive, feline, white-tailed deer

Severe acute respiratory syndrome coronavirus 2 (SARS-CoV-2) is an emergent zoonotic beta-coronavirus initially identified in late 2019 after human-to-human transmission within central China (1). By early 2020, the virus had caused a pandemic infecting millions of people and continues to circulate throughout the world. Like other human coronaviruses, it

1

is spread via aerosolized particles, leading to respiratory infections (1, 2). Infected individuals develop a range of symptoms from mild/asymptomatic infection to severe pneumonia-like disease (i.e., coronavirus disease [COVID]) (2). Sequence analysis of known SARS coronaviruses points to a bat origin with probable intermediate hosts prior to human adaptation (3–5). However, the exact intermediate host and factors that led to its zoonosis and establishment within humans are under investigation.

Secretion of SARS-CoV-2 is thought to be primarily via aerosolized particles with high viral loads in the lungs and nasopharyngeal secretions of infected individuals (6, 7). However, both viral RNA and infectious particles have been detected in fecal samples of acutely infected individuals. In the original SARS-CoV outbreak, there was documented fecal-oral transmission of infection (6, 8–12). Fecal to oral spread and shedding is a common route of transmission of other animal coronaviruses. Oropharyngeal viral RNA shedding of SARS-CoV-2 in humans lasts for ~17 days on average but persists up to 60 to 120 days in the respiratory tract and stool (13). Similarly, oropharyngeal secretion of infectious SARS-CoV-2 in cats appears to cease by 5 to 10 days postinfection (dpi) (14). Infected felids shed SARS-CoV-2 viral RNA in their feces for at least 5 dpi, but whether that represents infectious virus or a potential route of transmission is yet to be demonstrated (15).

Due to the multiple routes of spread and close contact with other species, transmission of SARS-CoV-2 from humans to animals is plausible (16). Human-to-animal and animal-to-animal transmission of SARS-CoV-2 has been documented or experimentally demonstrated. Companion animals such as cats and dogs are susceptible to experimental as well as natural infection from COVID-positive owners (14, 17–21). In addition, susceptible animals are capable of transmitting infection to cohoused animals (14, 22). In the case of minks, transmission from humans-to-minks and back to humans was demonstrated (23). This is similar to a situation at the Amoy Garden complex during the original SARS-CoV outbreak, where animal-to-human transmission occurred when an animal vector potentially contracted and spread SARS-CoV throughout the complex (24–26). Human transmission of SARS-CoV-2 to companion animals opens up the potential for spillover into wild animal populations. Indeed, transmission from humans to deer within North America has been proposed, as postpandemic deer were found to be seropositive in multiple states and SARS-CoV-2 genome was sequenced from lymph nodes (27–29). Human to animal transmission could contribute to the spread of SARS-like coronaviruses and the establishment of new reservoirs for recombination and the generation of future novel coronavirus outbreaks.

Infected humans and animals mount humoral responses to SARS-CoV-2 (13, 14, 30–32). In humans, SARS-CoV-2 antibodies arise within 5 to 14 days post-infection/symptom onset and peak around 17 to 20 dpi (13, 31, 33). For cats experimentally inoculated or naturally exposed to SARS-CoV-2, detectable antibody titers appeared by 7 to 14 dpi, peaking ~21 dpi (14). This matches anti-feline coronavirus (FCoV) responses, where high antibody levels can arise within ~9 dpi (34–36). Immunity to coronaviruses in cats is typically short-lived, with the average FCoV humoral responses lasting several months to 2 years (37). Anti-SARS-CoV-2 RBD responses in seropositive cats had similar declines in antibody titers only lasting around 4 to 5 months (38). However, humans infected with the initial SARS-CoV mounted robust responses detectable 1 to 2 years postexposure (39–41). The duration of anti-SARS-CoV-2 antibody responses is the subject of ongoing research, but natural exposure is unlikely to induce long-term or life-long immunity/seropositivity (42).

Major antigenic targets for SARS-CoV-2-infected individuals are the nucleocapsid, which is one of the most abundantly produced viral proteins (43), and spike protein, which is responsible for viral entry (44). The spike has high immunogenicity and diverges from other coronaviruses (32, 44, 45). Spike is composed of two subunits (S1/S2). The S1 subunit contains the receptor binding domain (RBD) responsible for binding to host ACE-2 and determining tropism/entry, while the S2 domain contains the fusogenic region of the spike (44, 45). SARS coronaviruses share very low similarity to

other coronaviruses within the spike protein (32), but antibodies against the S2 subunit can cross-react with common human coronaviruses (46–48). Cross-reactivity of the S1 subunit occurs at very low rates. Within the S1 region, the RBD is highly immunogenic and unique to SAR-COV/SARS-CoV-2 (32, 49). Serum from humans infected with common human coronaviruses such as OC43, NL63, and 229E failed to recognize the RBD from SARS-CoV-2 (32, 46, 49). Animals infected or immunized with other coronaviruses similarly fail to generate cross-reactive antibodies against SARS-CoV-2's RBD (32). For infected cats, SARS-CoV-2 seroconversion was not impacted by preexisting immunity against feline coronavirus (FCoV), an alpha-coronavirus with limited similarity to SARS-CoV-2 (38). Collectively, seropositivity against the RBD of SARS-CoV-2 is a specific marker of SARS-CoV-2 exposure and has led several groups to create highly specific indirect enzyme-linked immunosorbent assays (ELISAs) against SARS-CoV-2's RBD to screen for SARS-CoV-2 exposure (30, 32, 33). A final consideration of antibodies targeting the RBD is whether they are neutralizing or nonneutralizing (33, 50–53). For example, serum from humans and animals exposed to the original SARS-CoV were able to recognize the spike and RBD of SARS-CoV-2, while their cross-neutralization potential was variable (54, 55).

Despite limited similarity in the spike protein of SARS-CoV-2 versus common circulating coronaviruses, there are reports of prepandemic, preexisting SARS-CoV-2 reactive serum in humans (48, 49, 54). These cross-reactive antibodies represent a rare response to common human coronaviruses within conserved epitopes of SARS-CoV-2's spike protein (usually in the S2 region) with reports of ~0.6% prevalence of preexisting anti-RBD responses (46, 48, 49). Although there is increasing evidence for earlier timelines of SARS-CoV-2 spread among humans, preexisting seropositivity among other species has not been reported (38, 56–58). Indeed, even within central China, researchers failed to find evidence of SARS-CoV-2 exposure prior to the pandemic (38, 56, 58).

As SARS-CoV-2 spreads and encounter's new species, there is a need for monitoring local populations for SARS-CoV-2 transmission and the potential establishment of local reservoirs. Currently, we have a limited understanding of coronavirus reservoirs, spread, and recombination among diverse species. The original SARS outbreak in 2003 was a harbinger of the potential risk of crossover coronaviruses. At that time, animal coronavirus surveillance was a high priority. Unfortunately, this investment was not sustained. Our aim was to address whether SARS-CoV-2 is being introduced into companion animals of North America by tracking seroconversion using an in-house indirect ELISA against the RBD of SARS-CoV-2. We chose to focus on companion animals (i.e., cats and dogs), as they represent a significant source of human-animal interactions with potential for contact and further spillover into wild animal populations. Surprisingly, we found evidence of anti-RBD seropositive animals predating the pandemic by several months to years. Our study provides evidence for the existence and prevalence of SARS-CoV-2 serum reactivity prior to the current pandemic.

RESULTS

We developed an in-house ELISA to serologically screen companion animals based on a protocol developed at Mt. Sinai (30, 59). To examine cross-reactivity of our in-house anti-SARS-CoV-2 RBD indirect ELISA, we used polyclonal guinea pig serum raised against different animal coronaviruses (Fig. 1A). Consistent with previous reports, no cross-reactive antibodies for any of the common coronaviruses were found (18, 32, 38, 56). Only antibodies from SARS-CoV- or SARS-CoV-2-infected individuals reacted (Fig. 1A and B). Human serum collected from individuals prior to the SARS-CoV-2 pandemic or plasma from recovered SARS-CoV-2 donors was used to validate our ELISA screen (Fig. 1B). Receiver operator curve (ROC) analysis determined the positive cutoff threshold, using a value that gave highest specificity and sensitivity with prepandemic human serum and serum from confirmed SARS-CoV-2 infected individuals. ROC analysis was in agreement with the commonly used threshold determination method of three standard deviations above the mean negative value. Our assay based on RBD

A.

OD$_{450}$	α-TCoV	α-PRCoV	α-CCoV	α-FCoV	α-BCoV	α-SARS-CoV	α-SARS-CoV-2	Pre-Pandemic
25%	0.038	0.227	0.161	0.109	0.084	0.935	0.996	0.078
Median	0.048	0.253	0.193	0.159	0.102	1.008	1.000	0.088
Mean	0.058	0.258	0.199	0.173	0.127	1.051	1.000	0.095
75%	0.054	0.280	0.249	0.246	0.180	1.209	1.004	0.115

B.

Sensitivity = 96.96% (64/66)

Specificity = 95.45% (21/22)

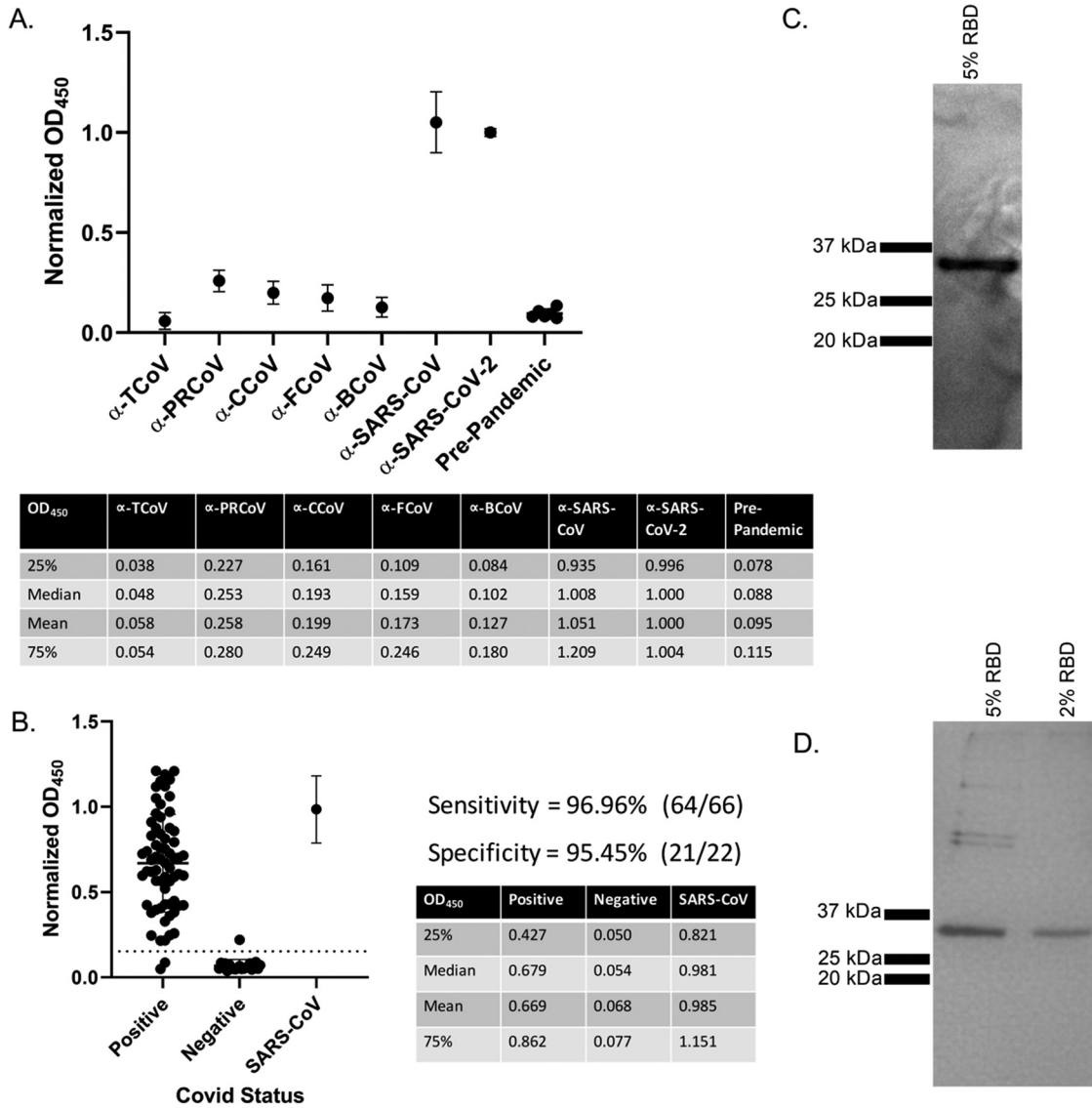| OD$_{450}$	Positive	Negative	SARS-CoV
25%	0.427	0.050	0.821
Median	0.679	0.054	0.981
Mean	0.669	0.068	0.985
75%	0.862	0.077	1.151

FIG 1 Anti-SARS-CoV-2 ELISA sensitivity and specificity. (A) Cross reactivity of anti-CoV antibodies against SARS-CoV-2 RBD. Polyclonal sera from guinea pigs immunized with common animal coronaviruses (turkey coronavirus, TCoV; porcine respiratory coronavirus, PRCoV; canine coronavirus, CCoV; feline coronavirus, FCoV; bovine coronavirus, BCoV) were used in a SARS-CoV-2 RBD indirect ELISA. Positive samples consisted of polyclonal serum from a SARS-CoV-2-infected patient and a monoclonal antibody to SARS-CoV (CR3022). The negative-control group comprised prepandemic human sera. Secondary antibodies were either anti-human IgG (1:10,000) (Rockland Immunochemicals, USA) or anti-guinea pig IgG (1:10,000) (Life Technologies Corp., USA). Bars represent the mean and standard deviation ($n > 3$ for all samples). (B) ELISA validation using 66 human COVID-positive plasma and 22 negative serum samples. Human antibodies against the SARS-CoV-2 RBD were detected with an indirect RBD-specific ELISA. Secondary antibody was the anti-human IgG (1:10,000) (Rockland Immunochemicals, USA). ROC analysis determined the positive OD$_{450}$ cutoff value (dashed line). Positive plasma samples were donated by COVID-recovered patients, and prepandemic serum samples were the negative controls. Based on the experimentally determined cutoff value, 64 of the 66 positive samples were anti-RBD positive, giving a sensitivity value of 96.96%. All but one of the negative samples were below the cutoff value for a specificity of 95.45%. The adjacent tables list the first and third quartiles along with mean and median OD$_{450}$ values of COVID-positive and -negative human samples. Bars represent the mean and standard deviation ($n > 3$). (C) Anti-6×His Western blot on HEK-293T17 purified RBD from 5% serum conditions. Samples were run on a 12% denaturing SDS-PAGE gel. Protein was transferred to nitrocellulose and probed with anti-6×His antibody at 1:10,000 (Proteintech, USA). White light and chemiluminescent images were overlaid and from left to right, are ladder (lane 1) and purified RBD (lane 2). (D) Silver stain of purified recombinant SARS-Cov-2 RBD produced in HEK-293T17. From left to right, ladder, HEK-RBD under 5% serum conditions, HEK-RBD from 2% serum conditions. Samples were denatured and run on a 12% SDS-PAGE gel and silver-stained (Thermo Fisher Scientific, USA). For panels B and C, representative data are shown.

screening showed high sensitivity (96.96%) and specificity (95.45%) with 66 SARS-CoV-2 samples and 22 pre-SARS-CoV-2 samples (Fig. 1B). While Stadlbauer et al. (59) performed two diagnostic ELISAs, one with RBD and the other with full-length spike, our results using only the RBD-based screen are in good agreement with their published

data. Others have also demonstrated the accuracy of an RBD-only-based ELISA (33, 38). A Western blot using an anti-6×His antibody (Fig. 1C) shows the expected size of purified RBD with a single band of ~32 kDa. This shows that our isolated RBD is the correct size and runs as a monomer. Silver stain of the same affinity-purified SARS-CoV-2 RBD demonstrates relative purity (Fig. 1D). However, there are copurified proteins present at lower levels.

To establish a baseline for future SARS-CoV-2 screening of companion animals, 128 prepandemic feline serum samples collected prior to December 2019 were retrospectively screened using our in-house ELISA. A total of 19 samples were of a known FCoV serological status, with the remaining 109 of unknown FCoV status. Following the same protocol used for screening human serum samples (Fig. 1), feline samples were tested for antibodies against SARS-CoV-2's RBD (Fig. 2A). There were two batches tested, serum samples from feral cats in East Tennessee collected from 2007 to 2012 ($n = 36$) and convenience samples from client-owned cats undergoing routine blood work (listed as prepandemic) ($n = 92$) (Fig. 2A). As expected, SARS-CoV-2 experimentally infected cats (14) tested positive with high relative optical density at 450 nm (OD_{450}) and normal cat serum (i.e., negative control), with very low relative OD_{450} (Fig. 2A). Despite predating the pandemic, 52% (67/128) of the cat samples tested positive for antibodies against SARS-CoV-2 RBD. This is surprising, as there was a lack of high cross-reactivity in guinea pigs immunized with FCoV in Fig. 1A. Several reports also showed a lack of similarity and cross-reactivity between alpha coronaviruses and SARS-CoVs (18, 32, 38, 56). Indeed, two other groups found that preexisting immunity to FCoV had no impact on seropositivity of feline samples (38, 58). To ensure that the positive ELISA results were specific to the RBD and not to a copurified protein, Western blot analysis was carried out using serum from a positive sample (Fig. 2B). Positive cat serum bound an ~32-kDa protein, the size of the RBD protein (Fig. 1C). Notably, normal cat serum did not react with any other protein despite the presence of copurified proteins. To further show the specificity of the anti-RBD response, we titrated seropositive and seronegative samples. Starting with serum from cats experimentally infected with SARS-CoV-2 (Fig. 2A) and normal cat serum, we saw a normalized OD_{450} >3 standard deviations above the negative control (i.e., normal cat serum) at all dilutions. This gives a titer of >8,100 (Fig. 2C). Then, 17 seropositive and 10 seronegative pre-2020 cat samples were titrated and assayed in our ELISA (Fig. 2D). Titers ranged from 900 to 8,100, with a median titer of 2,700 demonstrating both a high anti-SARS RBD prevalence and titer. Titrations of these earlier seropositive and seronegative feral cat samples have a similarly high titer (Fig. 2E) (median titer, 8,100) which is on par with the prepandemic samples. The area under the curve (AUC) for all groups is shown to the right side of their respective titration. AUC analysis of the titrated samples showed a significant difference between all positive and negative samples.

Following the surprising presence and prevalence of anti-RBD responses in prepandemic cats, we explored the epidemiological characteristics of our samples. Prepandemic convenience samples were submitted to the University of Tennessee for diagnostic testing of feline herpesvirus, feline calicivirus, and FCoV. Age, sex, and location of seropositive and seronegative samples are shown in Table 1. Both seropositive and seronegative samples had a mean age of >3 years with no difference between the groups and contained similar ratios of male:female animals (Table 1). Seropositive samples were found in disparate geographic locations from opposite coasts of the United States (i.e., New York to California [Table 1]). This observation indicates that seropositivity is not confined to a single geographic region (e.g., East Tennessee). Based on our limited sampling, we were unable to identify any unique characteristic or identifier for seropositive versus seronegative samples.

With our discovery of preexisting antibodies against SARS-CoV-2's RBD, it was pertinent to examine samples from dogs, another companion animal with high human contact. Serum samples from dogs ($n = 36$) were collected and retrospectively screened as part of a tick study during a 7-month period beginning in January 2020 and extending into July 2020. These samples are considered postpandemic because the time frame
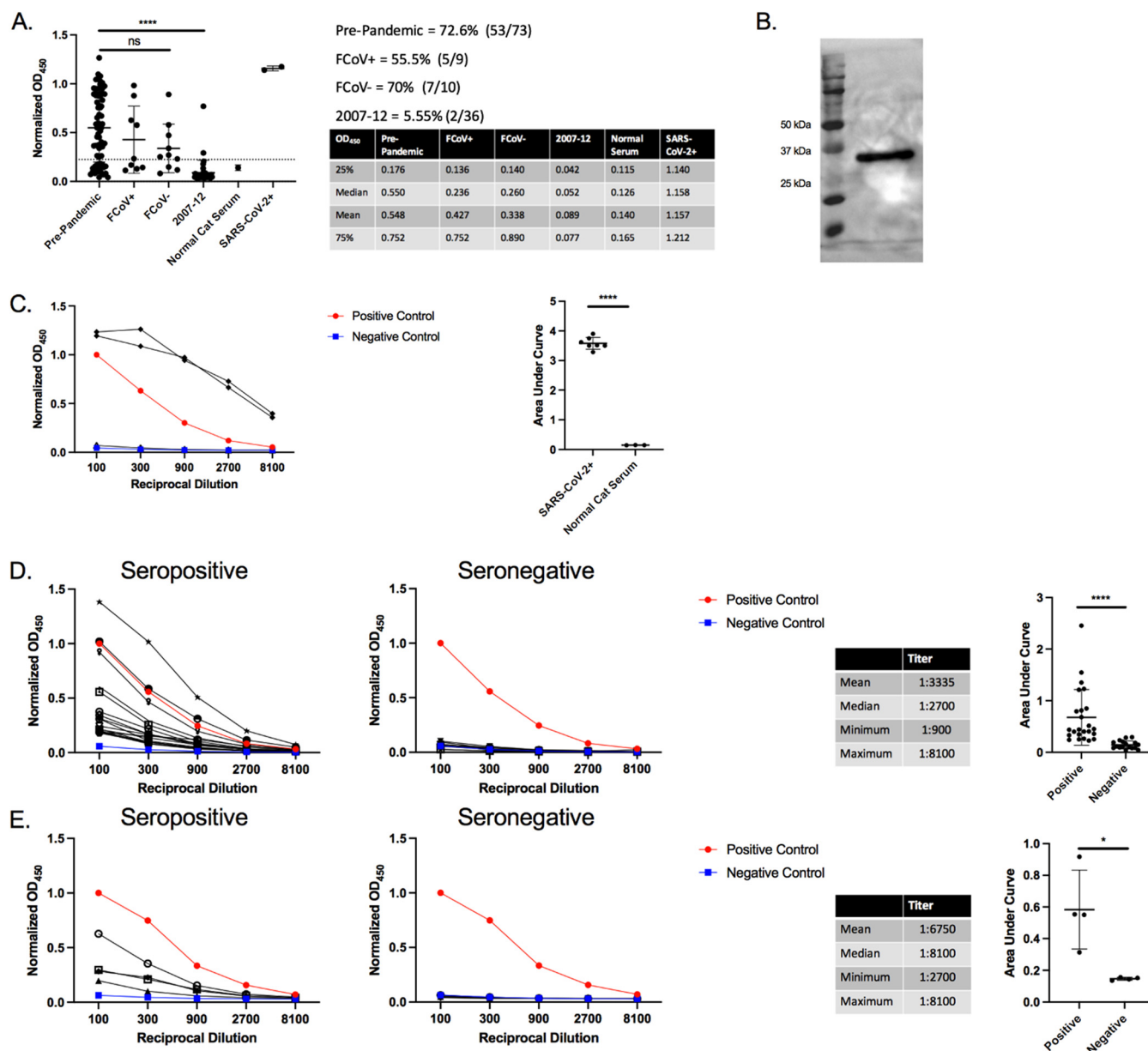
FIG 2 Prepandemic feline antibodies cross-react with SARS-CoV-2 RBD. (A) ELISA results of cat serum RBD reactivity. A total of 93 prepandemic feline serum samples were tested for reactivity in our anti-RBD ELISA with anti-felid IgG secondary antibody (1:10,000) (Invitrogen, USA). Cutoff values were determined by receiver operator curve (ROC) analysis. OD_{450} values for samples in each group were plotted, with the dotted line representing the positive threshold. Two sets of prepandemic cat samples were collected. Prepandemic convenience samples ($n = 73$) were collected in local clinics and sent to the University of Tennessee for diagnostic testing or during feral cat studies (2007 to 2012) ($n = 36$). Prepandemic convenience samples were subdivided into feline coronavirus-positive (FCoV+) and -negative (FCoV–) subgroups. Normal cat serum (Jackson ImmunoResearch Laboratories, USA) serves as the negative control, and SARS-CoV-2+ serum from two cats experimentally inoculated with SARS-CoV-2 serves as positive controls. The side table lists the first and third quartiles and mean and median OD_{450} values for all samples. Bars represent the mean $\pm$ standard deviation ($n > 3$ for all samples). (B) Western blot of purified RBD using serum from a single positive cat sample. Purified RBD was run under denaturing conditions and blotted onto nitrocellulose. The RBD blot was first probed with cat serum from an ELISA positive sample (1:20 dilution) followed by anti-felid IgG-HRP conjugated antibody (1:10,000 dilution) (Invitrogen, USA). White light and chemiluminescent images were overlaid. Lane 1 is the molecular weight ladder and lane 2 is purified RBD. (C to E) Titration of seropositive and seronegative serums assessed via RBD ELISA. OD_{450} values were plotted against the reciprocal dilution. Samples were considered positive if they were 3 standard deviations above the negative average for each dilution. Anti-RBD titer was designated the last dilution above the negative cutoff. Positive controls were human COVID-positive serum, and negative controls were normal human and cat serum (Jackson ImmunoResearch Laboratories, USA). Statistics for the positive sample titrations are included in the table along with AUC analysis. (C) Serum from two SARS-CoV-2-infected cats (red circles) and normal cat serum (blue squares) were titrated in an anti-RBD ELISA. (D) Titration of 17 seropositive and 10 seronegative, prepandemic cat samples. (E) Titration of four seropositive and seronegative cat samples collected from 2007 to 2012. For panels A and B, representative data are shown. For panel A, Tukey's one-way ANOVA with multiple comparisons was performed. For panels C, D, and E AUC analysis and Student's one-tailed t test with Welch's correction were performed. *, $P < 0.05$; **, $P < 0.01$; ***, $P < 0.001$.

TABLE 1 Characteristics of feline samples

Characteristic	No. seropositive	%	No. seronegative	%
Age				
Total no. of samples	58		15	
Avg age of feline (yrs ± SD)	3.56 ± 3.67		3.87 ± 4.37	
<1 yr	15	25.86	5	33.33
1–3 yrs	22	37.93	4	26.67
4–6 yrs	10	17.24	2	13.33
>6 yrs	11	18.97	4	26.67
Sex				
Total no. of samples	56		19	
Male	30	53.57	12	63.16
Female	26	46.43	7	36.84
Location				
Total no. of samples	62		21	
TN	10	16.12	7	33.33
NY	19	30.64	9	42.85
CA	27	43.54	5	23.8
MA	4	6.45	0	0
SC	1	1.61	0	0
WI	1	1.61	0	0

straddles the arrival of SARS-CoV-2 in East Tennessee (~March 2020). The initial ELISA screen identified 97% seropositivity in the dog samples (Fig. 3A), with only 1 sample falling below the cutoff established on human serum. Surprisingly, serum from purpose-bred research animals housed at the University of Tennessee also showed high levels of reactivity (Fig. 3A). This raised suspicion about the specificity of the response. To address this, Western blot analysis with canine serum (Fig. 3B) identified a protein other than the RBD (see the ~32-kDa protein in Fig. 1C and 2B). The canine serum recognized an ~60- kDa protein which is likely a copurified protein present after RBD purification and is faintly seen in the silver-stained gel in Fig. 1D. This copurified protein was not detected in the blots performed for Fig. 1C and 2B using anti-6×His monoclonal antibody and cat serum, respectively. Although there is a possibility that canine serum recognizes an oligomer of RBD (60), based on Fig. 1C, the anti-6×His antibody does not detect any protein of >32 kDa, eliminating this possibility.
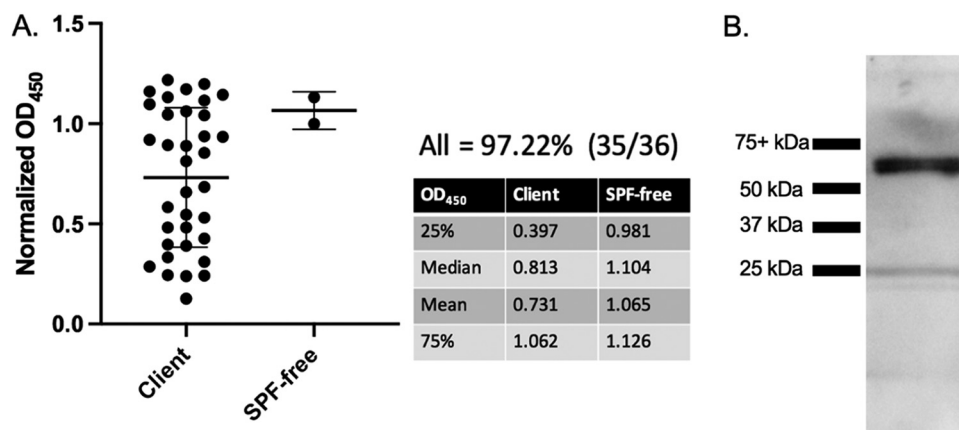

FIG 3 Dog serum cross-reacts to a copurified protein. (A) Anti-SARS-CoV-2 RBD ELISA with dog serum. Serum from 36 client-owned and two purpose-bred research dogs were tested in an anti-RBD ELISA with anti-canine IgG secondary HRP (1:10,000) (Bethyl Laboratories, USA). The table to the right lists the first and third quartile, median, and mean OD_{450} values for all samples. Bars represent the mean ± standard deviation ($n > 3$). (B) Western blot of purified RBD using serum from a positive dog sample. Purified RBD was probed with dog serum from an ELISA positive sample (1:20 dilution) followed by anti-canine IgG HRP (1:10,000 dilution) (Bethyl Laboratories, USA). White light and chemiluminescent images were overlaid. Lane 1 (from left to right), ladder; lane 2, purified RBD. For all figures, representative data are shown.
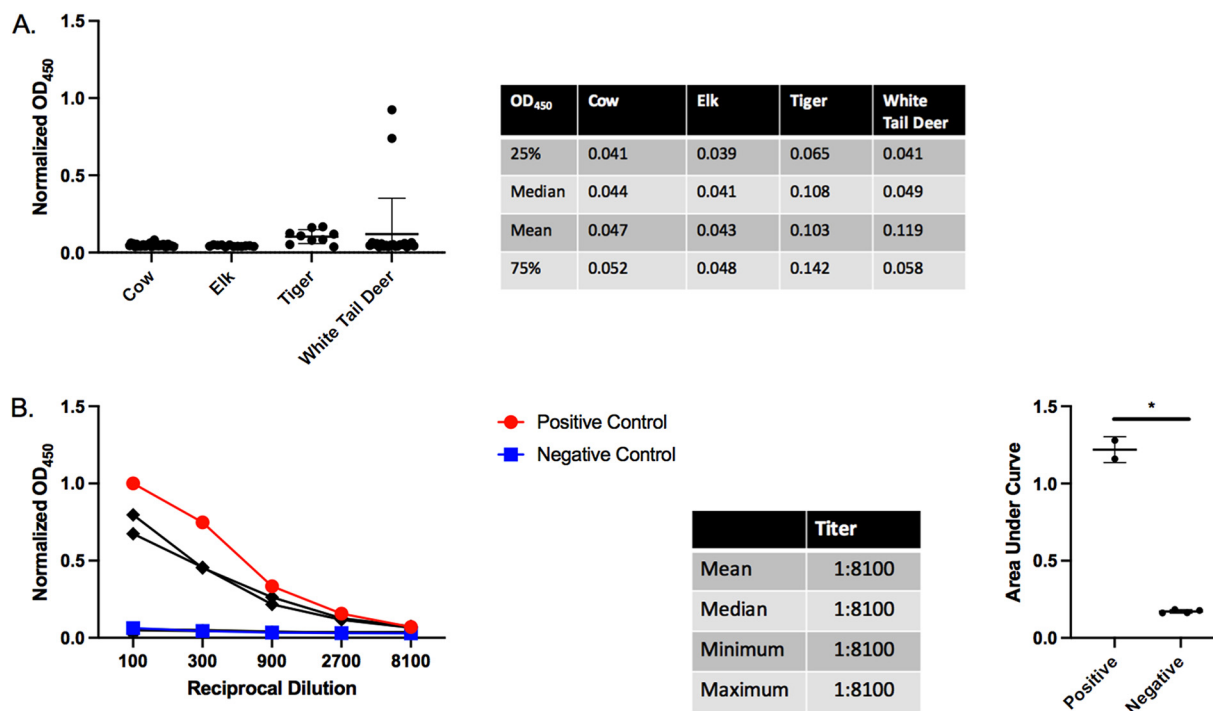
FIG 4 Serological testing of other regional animals. (A). Anti-SARS-CoV-2 RBD ELISA with bovine, elk, tiger, and deer serum; 33 prepandemic East Tennessee cows, 12 postpandemic East Tennessee elk, 9 prepandemic East Tennessee tigers, and 22 postpandemic South Carolina deer serum samples were tested for anti-RBD antibodies. Species-specific secondary antibodies were used at the following dilutions: anti-bovine, 1:250 (Bethyl Laboratories, USA); anti-elk/deer, 1:250 (KPL, USA); anti-tiger/cat, 1:10,000 (Invitrogen, USA); and anti-deer, 1:250 (KPL, USA). Bars represent the mean ± standard deviation ($n > 3$ for all samples). (B) Titration of two seropositive (red circles) and four seronegative (blue squares) deer samples. OD_{450} values are plotted against the reciprocal dilution of each sample. Samples were considered positive if they were 3 standard deviations above the negative average for each dilution. Positive and negative controls were human COVID-positive and -negative samples, respectively. Statistics for the positive sample titrations are included in the table. The AUC analysis for titrations of deer ELISA positive and negative samples is shown to the right. For all figures, representative data are shown. For AUC analysis Student's one-tailed t test with Welch's correction was performed. *, $P < 0.05$; **, $P < 0.01$; ***, $P < 0.001$.

Following our observation of high levels of anti-SARS-CoV-2 RBD antibodies in North American cats, we began examining other regional animals. Serum samples from Tennessee resident, prepandemic cows ($n = 33$) and tigers ($n = 9$), postpandemic East Tennessee elk ($n = 12$), and postpandemic South Carolina white-tailed deer ($n = 22$) were tested for anti-SARS-CoV-2 RBD antibodies (Fig. 4A). Of the four species tested, only the deer from South Carolina showed any seropositive samples (2/22). Serum titrations show the two seropositive samples have a high titer of >8,100 (Fig. 4B), and the AUC of the titrations show a significant difference between seropositive and negative deer samples (Fig. 4C). Unfortunately, due to limited sample volume, we were unable to run Western blots to demonstrate the specificity for the RBD protein. The deer are postpandemic and could represent recent transmission of SARS-CoV-2 into the deer population. Although these animals probably have had limited contact with humans, white-tailed deer are susceptible to and capable of transmitting SARS-CoV-2 (61). Another possibility is that this species was exposed to the same etiological agent as our prepandemic seropositive cats.

To address whether our ELISA-positive animal samples can neutralize SARS-CoV-2 infections, we measured the ability of cat serum to block the interaction of the spike protein with the human ACE-2 (hACE-2) receptor using a commercially available flow cytometry-based bead assay. In this assay, neutralization is characterized as the decrease in fluorescence when antibodies block the fluorescently labeled SARS-CoV-2 S1 subunit from binding to hACE-2 conjugated beads (Fig. 5A). Because this assay is not species specific or immunoglobulin type dependent, it is applicable for assessing both human and feline serum. The internal antibody control shows a decrease in
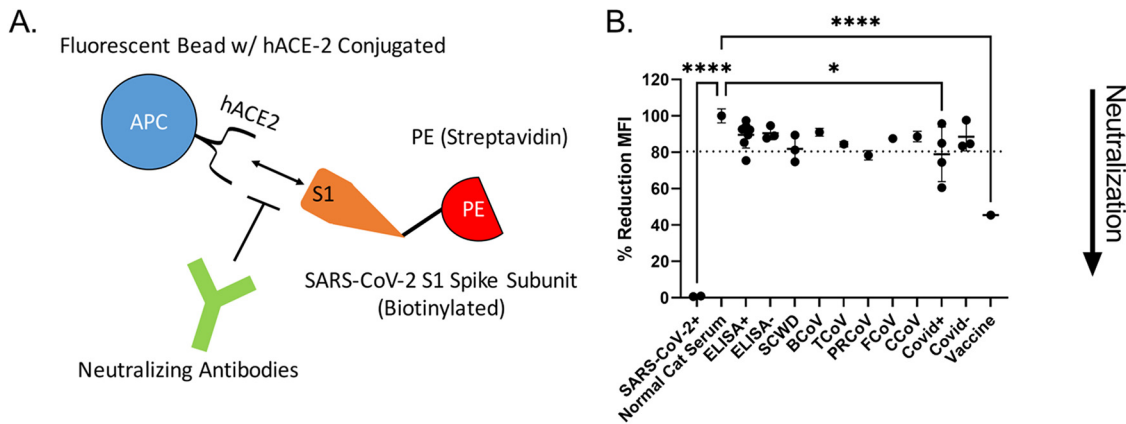
FIG 5 Neutralization assays. (A) Schematic of the neutralization assay. Neutralization is measured as the decrease in binding of phycoerythrin (PE)-labeled SARS-CoV-2 S1 subunit to human ACE-2 conjugated beads. Addition of neutralizing antibodies results in a decreased mean fluorescent intensity (MFI) as measured by flow cytometry. (B) Neutralization of SARS-CoV-2 S1 subunit interaction with hACE2. Serum from several ELISA positive and negative cats (ELISA+ and ELISA–, respectively), serum from South Carolina white-tailed deer (SCWD, 2 ELISA positive and 1 negative), mice immunized with other common coronaviruses (BCoV, bovine coronavirus; TCoV, turkey coronavirus; PRCoV, porcine respiratory coronavirus; FCoV, feline coronavirus; CCoV, canine coronavirus), and human serum samples (Covid+, convalescent plasma from Covid+ humans; Covid–, pre-SARS-CoV-2 serum samples; vaccine, serum postvaccination against SARS-CoV-2 spike protein) were used. SARS-CoV-2-infected cats and normal cat serum served as positive and negative controls, respectively. Data were normalized to normal cat serum representing 100% binding of SARS-CoV-2 S1 subunit to hACE2 beads. ROC analysis was used to generate a positive reduction threshold (dotted line). Each point is an average of 2 replicates. Tukey's one-way ANOVA with multiple comparisons was used to analyze experimental groups. *, $P < 0.05$; ****, $P < 0.0001$.

fluorescence corresponding to levels of neutralizing monoclonal antibody against SARS-CoV-2. Serum from experimentally infected cats showed potent neutralization at a 1:100 dilution. However, only one ELISA-positive, prepandemic cat sample showed neutralization (Fig. 5B). One of the seropositive white-tailed deer samples and a single serum sample from mice immunized with porcine respiratory coronavirus (PRCoV) also showed slight neutralization, clearing the determined ROC threshold/cutoff value (Fig. 5B). Notably, we were unable to detect high levels of neutralization/neutralizing antibodies even in several of the human convalescent-phase serum samples (Fig. 5B).

Because cross-reactivity of antibodies to SARS-CoV-2 RBD independent of SARS-CoV-2 infection has not been previously reported in felines, we suspected that the etiological agent could be another coronavirus (38, 58). Fecal samples were collected from healthy East Tennessee cats and screened for coronaviruses using pan-coronavirus primers amplifying conserved regions of the RNA-dependent RNA polymerase (RdRp), helicase (Hel), and spike (S) genes (62). Coronavirus viral RNA, whether common animal coronavirus or SARS-like coronavirus, is potentially shed in feces (8, 9, 11, 13). Collection of fecal samples used a noninvasive collection method, and SARS-CoV-2 has been reported to have prolonged shedding within fecal samples of humans (8, 9, 11, 13). Out of 30 samples, 15 (50%) tested positive for at least one loci, with most yielding positive results for multiple loci (Table 2). Not surprisingly, sequences cluster within the alpha-coronavirus group and with high similarity to previously identified FCoV strains. When all five loci were aligned and concatenated together, the maximum-likelihood phylogenetic tree placed the concatenated coronavirus sequences within the alpha-coronavirus lineage, closely related to FCoV (Fig. 6A). We were unable to amplify or identify any sequences which resemble SARS-like coronaviruses or beta-coronaviruses. Partial sequencing of the S1 region was able to amplify the RBD from several coronavirus RNA-positive samples. The sequenced RBDs were again highly similar to FCoV based on a maximum-likelihood phylogenetic tree (Fig. 7A). Along with the phylogenetic tree, a similarity matrix demonstrates high RBD similarity between previous FCoV strains and those sequenced here (~80%) (Fig. 7B). The RBD from these fecal samples displays low similarity to beta-coronaviruses such as Middle East respiratory syndrome (MERS), SARS-CoV, and SARS-CoV-2 (~30%) as previously reported (Fig. 7B).

TABLE 2 Fecal coronavirus screening information[a]

Sample	RdRp1	RdRp2	Spike1	Spike2	Spike3	Helicase	Location	Accession no.[b]
CP-20-01		■		■		■	Jefferson County, TN, USA	MZ220722–MZ220724
CP-20-02		■		■		■	Washington County, TN, USA	MZ220725–MZ220727
CP-20-03							TN, USA	NA
CP-20-04	■	■				■	Monroe County, TN, USA	MZ220728–MZ220730
CP-20-05							TN, USA	NA
CP-20-06							Sullivan County, TN, USA	NA
CP-20-07	■	■		■		■	Grainger County, TN, USA	MZ220731–MZ220734
CP-20-08		■		■			Monroe County, TN, USA	MZ220735
CP-20-09		■		■		■	Sullivan County, TN, USA	MZ220736–MZ220738
CP-20-10							Washington County, TN, USA	NA
CP-20-11							Jefferson County, TN, USA	NA
CP-20-12	■	■	■	■			Monroe County, TN, USA	MZ220739–MZ220742
CP-20-13	■	■		■			Grainger County, TN, USA	MZ220743–MZ220745
CP-20-14							Jefferson County, TN, USA	NA
CP-20-15							Sullivan County, TN, USA	NA
CP-20-16							Sevier County, TN, USA	NA
CP-20-17							Cocke County, TN, USA	NA
CP-20-18							Hamblin County, TN, USA	NA
CP-20-19			■	■			Washington/Sullivan County, TN, USA	MZ220746–MZ220747
CP-20-20				■			Hamblin County, TN, USA	MZ220748
CP-20-21							Washington/Sullivan County, TN, USA	NA
CP-20-22							Grainger County, TN, USA	NA
CP-20-23		■		■			Jefferson County, TN, USA	MZ220749–MZ220750
CP-20-24							Jefferson County, TN, USA	NA
CP-20-25							Grainger County, TN, USA	NA
CP-20-26	■	■	■	■		■	Grainger County, TN, USA	MZ220751–MZ220755
CP-20-27	■	■		■			Grainger County, TN, USA	MZ220756–MZ220759
CP-20-28		■					Washington/Sullivan County, TN, USA	MZ220760
CP-20-29							TN, USA	NA
CP-20-30	■					■	Grainger County, TN, USA	MZ220761–MZ220762

[a]Sample IDs were assigned to deidentified fecal samples from healthy cats. RNA was extracted from each and PCR screened for amplification of 6 coronavirus loci across 3 conserved genes (RdRp, spike, and helicase). Positive amplification and sequencing are shown by a black shaded box. Out of 30 samples, 15 were positive for at least 1 coronavirus loci. Animals originated from multiple East Tennessee counties, and when known, the exact county of origin is listed. Accession numbers for each sample are shown to the right.

[b]NA, not applicable, no amplification.

DISCUSSION

We have employed serological screening as a method to detect potential SARS-CoV-2 exposure in animal populations. Tracking active viral spread in wild and domesticated animals in real-time via sequencing and reverse transcriptase quantitative PCR (RT-qPCR) is expensive and low throughput. In addition, the unknown transient nature of viral shedding from different secretions/locations makes this type of surveillance prohibitively expensive with no guarantee of identifying a virus. Serological detection of antibodies against SARS-CoV-2 is comparatively high-throughput and inexpensive while still maintaining sensitivity. A downside of this methodology is the lack of an up-to-date picture of cross-species transmission, as serology trails initial infections by several days to weeks (22, 33). On the other hand, due to the lowered cost of serological testing, there is a compensatory increase in testing capability allowing a broader swath of animals and regions to be sampled with more frequent resampling to track spillover into new species. Our adapted protocol yields recombinant SARS-CoV-2 RBD protein, allowing production of a low-cost indirect anti-RBD ELISA. The recombinant RBD was sufficient for serological screening via ELISA and is amenable to most labs with prior tissue culture capabilities and does not require large initial investments in cell lines, culture media, or specialized incubators. We validated our method demonstrating low cross-reactivity with other common animal coronaviruses (Fig. 1A) and >95% sensitivity and specificity on human serum samples (Fig. 1B).

For the seropositive samples identified in our study, mean titers for positive cat samples were relatively high at ~2,700 (Fig. 2E and G), which based on reported rapid declines in anti-RBD responses for SARS-CoV and FCoV, points to exposure within the

past few years (37, 38, 40). Further, based on FCoV studies, animals with high titers typically correlate with active viral shedding and spread within a household, which highlights a potential overlap between seropositivity and viral shedding (37). This is in stark contrast to SARS-CoV-2 serosurveys on pre- and postpandemic feline samples from Central China. They found no evidence of exposure before the outbreak, but also, positivity levels postpandemic were significantly lower than those shown here (~12% in Central China versus >50% in the United States) (Fig. 2A) (38, 58). OD_{450} and titers of prepandemic seropositive cat samples, while high, were lower than SARS-CoV-2-experimentally inoculated cats (6 weeks postinfection) (Fig. 2A, C, E, and G). This likely represents a natural decline in titer over time for the environmental samples but could also represent lower titers of cross-reactive antibodies from another coronavirus.

Unfortunately, dog serum was shown to bind to a copurified protein (Fig. 3B), leaving us unable to utilize our assay for examining cross-species transmission of SARS-like coronaviruses to canines. We can show that recombinant RBDs produced and purified by groups at both Mt. Sinai and Emory contain copurified proteins at approximately the same size as those shown in Fig. 1A (30, 33). As such, screens for SARS-CoV-2 exposure in canines would likely require producing and purifying the RBD using a different strategy that eliminates non-RBD protein contamination. Recently, both SARS-CoV-2's RBD and soluble full-length spike have been produced and purified in plants (63). This alternative method may prove useful for animal SARS-CoV-2 screening by reducing or eliminating false positives due to copurified proteins.

After the discovery of prepandemic seropositive cats, we examined other commercial (cow) and convenience samples from local wild species (deer, elk, tiger) (Fig. 4A). Out of 22 white-tailed deer from South Carolina, 2 (9%) were positive for antibodies against the RBD (Fig. 4B). Unlike our cat samples, the two seropositive deer could represent transmission of SARS-CoV-2 into the local deer population because these samples were collected postpandemic. Interestingly, a recent report showed that ~40% of white-tailed deer from 4 states (Illinois, Michigan, New York, and Pennsylvania) were positive for SARS-CoV-2 antibodies (29). Seropositive animals were only observed from 2019 onward, with prepandemic deer testing negative on their SARS-CoV-2 neutralization assay. This information supports our finding in South Carolina deer (Fig. 4). SARS-CoV-2 sequences were also recently isolated from the retropharyngeal lymph nodes of wild and captive deer (27, 28). The dominant genotype of deer-isolated SARS-CoV-2 genotypes closely corresponded to those circulating within humans at the time, pointing to potential rapid transmission from humans to animals (28). This highlights the importance of the One Health Initiative to provide information on the potential exposure and spillover into other species and the question of whether there is recombination with native coronaviruses occurring to generate new variants or establishment of new reservoirs in North America. Further work is needed to determine the prevalence, spread, and identity of SARS and other coronaviruses circulating within North American deer and associated species.

That samples from cats experimentally infected with SARS-CoV-2 displayed potent neutralization (Fig. 5B) is unsurprising because of their high ELISA titers (Fig. 2C). These samples were collected at ~8 weeks postinfection and likely represent peak titer and neutralization capacity (14). Neutralization of SARS-CoV-2 S1 subunit was variable for environmental feline ELISA-positive samples (Fig. 5B). There was no significant difference in mean fluorescent intensity (MFI)/neutralization between the anti-RBD seropositive and seronegative feline samples (Fig. 5B). Even sera from convalescent, COVID-recovered individuals showed no to minimal neutralization (Fig. 5B). Several groups have found that not all anti-RBD responses generate neutralizing antibodies (50–53, 64). Indeed, even in convalescent-phase serum, high levels of RBD recognition do not guarantee high neutralizing titers, consistent with our own observations (Fig. 5B) (50). Based on ELISA and neutralization results (Fig. 2A and 5B), we suspect that these animals contain antibodies recognizing SARS-CoV-2's RBD but likely bind to nonneutralizing epitopes of the RBD domain.
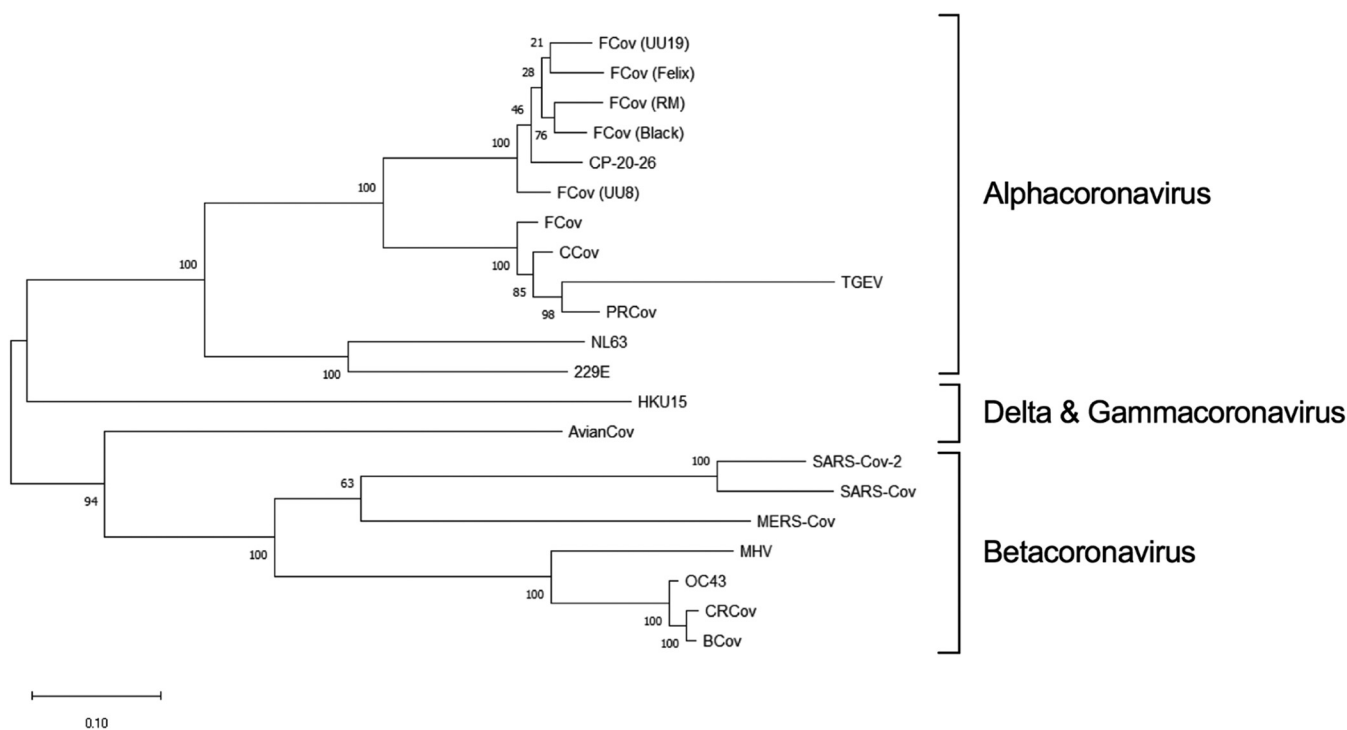
FIG 6 Pan-coronavirus screen of East Tennessee felines. Fecal samples from healthy cats were collected and screened for conserved coronavirus sequences. Phylogenetic trees were generated consisting of the following common human and animal coronaviruses: CRCoV (canine respiratory coronavirus), BCoV (bovine coronavirus), OC43 (human beta-coronavirus), MHV (murine hepatitis virus), MERS-CoV (Middle East respiratory coronavirus), SARS-CoV-2 (severe acute respiratory coronavirus-2), SARS-CoV (severe acute respiratory coronavirus), AvianCoV (duck coronavirus), NL63 (human alphacoronavirus), 229E (human alphacoronavirus), TGEV (transmissible gastroenteritis virus), PRCoV (porcine respiratory coronavirus), FCoV (feline coronavirus strains UU19, Felix, RM, Black, and UU8), CCoV (canine coronavirus), HKU15 (porcine delta-coronavirus), as well as a locally identified coronavirus (CP-20-26). Sequences from five coronavirus loci were independently aligned, trimmed, and concatenated. Concatenated sequences were aligned, and phylogenetic trees were generated with the maximum-likelihood method with bootstrap analysis in MEGA X. Bootstrap values for each branch are shown with lengths to scale. Coronavirus lineages are annotated on the tree.

Because ~50% of cats surveyed were seropositive, we reasoned that isolation of the suspected infectious agent or coronavirus might be possible. Based on fecal viral RNA shedding following animal coronavirus infections, PCR amplification with universal coronavirus primers was used to screen for potential causative agents of anti-RBD seropositivity. This allowed for noninvasive testing and isolation of coronavirus RNA from infected cats. In line with previous studies on other wild animals, we did not identify any nonalphacoronaviruses circulating in felines (65–68). The coronavirus sequences that were isolated and sequenced likely represent normal circulating FCoVs (Fig. 6). Due to the opportunistic nature of our sampling, we were unable to obtain any paired blood and fecal samples from the same animal. As such, we are unable to conclude whether the cats with identified FCoVs would produce cross-reactive antibodies against SARS-CoV-2's RBD. However, based on our ELISA results in Fig. 1A and 2A showing no correlation with SARS RBD antibodies and FCoV infection, we would suspect not. Furthermore, as we did not know when the seropositive cats were exposed (i.e., cats could have been infected potentially years prior to any fecal sampling), fecal sampling and sequencing would not detect a novel coronavirus if it had been cleared. Following the identification of coronavirus-positive fecal samples, we attempted to amplify and sequence the entire RBD region from positive samples to look for similarity to SARS-CoV-2 or SARS-like viruses. Large portions of the S1 region spanning the RBD were sequenced and contained RBD regions similar to previously isolated FCoV strains (Fig. 7), with no similarity to SARS or betacoronaviruses.

The current study demonstrates cross-reactivity of prepandemic feline samples with the RBD of SARS-CoV-2. Our indirect ELISA screen has provided evidence for seropositivity of serum from North American cats and deer to a SARS-CoV-2 protein previously
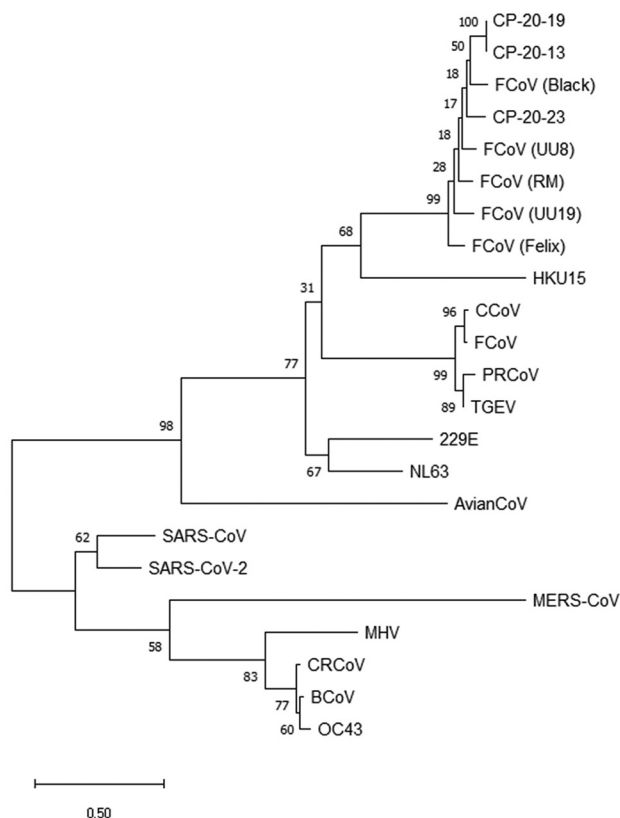
Percent Similarity	MERS-CoV	SARS-CoV	SARS-CoV-2	CP-20-23	CP-20-19	CP-20-13	FCoV (Black)	CCoV	FCoV	PRCoV	TGEV	229E	NL63
MERS-CoV	100												
SARS-CoV	32.2	100											
SARS-CoV-2	38.05	69.86	100										
CP-20-23	32.29	26.27	29.9	100									
CP-20-19	33.76	26.75	30.14	87.07	100								
CP-20-13	33.76	26.75	30.14	87.07	100	100							
FCoV (Black)	32.29	25.54	28.23	86.56	87.76	87.76	100						
CCoV	29.91	33.41	29.81	45.27	45.96	45.96	44.06	100					
FCoV	29.17	33.41	29.81	46.3	45.96	45.96	44.75	96.94	100				
PRCoV	30.34	34.14	30.53	45.61	46.64	46.64	44.92	88.1	88.78	100			
TGEV	31.01	34.14	31.49	45.96	46.81	46.81	45.09	91.67	91.67	94.9	100		
229E	32.02	31.52	28.47	45.17	44.05	44.05	42.19	45.54	44.98	45.54	44.98	100	
NL63	33.27	31.02	31.03	52.41	51.48	51.48	50	49.91	49.17	48.8	48.61	57.55	100

FIG 7 RBD coronavirus screen of East Tennessee felines. (top) Fecal samples from healthy cats were collected and screened for S1/RBD coronavirus sequences. Phylogenetic tree consisting of common human and animal coronaviruses: CRCoV (canine respiratory coronavirus), BcoV (bovine coronavirus), OC43 (human betacoronavirus), MHV (murine hepatitis virus), MERS-CoV (Middle East respiratory coronavirus), SARS-CoV-2 (severe acute respiratory coronavirus-2), SARS-CoV (severe acute respiratory coronavirus), AvianCoV (duck coronavirus), NL63 (human alpha-coronavirus), 229E (human alphacoronavirus), TGEV (transmissible gastroenteritis virus), PRCoV (porcine respiratory coronavirus), FcoV (feline coronavirus strains UU19, Felix, RM, Black, and UU8), CCoV (canine coronavirus), HKU15 (porcine deltacoronavirus), as well as locally identified coronaviruses (CP-20-13, CP-20-19, and CP-20-23). Sequences from the S1 region were aligned and trimmed. Maximum-Likelihood phylogenetic trees were generated with bootstrap analysis in MEGA X. Bootstrap values for each branch are shown with lengths to scale. (Bottom) Percent similarity matrix of select coronaviruses. Aligned and truncated RBD regions from the shown coronaviruses were analyzed via Clustal Omega to determine the percent identity matrix.

shown to be highly specific to SARS coronaviruses (32, 38, 46, 49). This is the first study to demonstrate seropositivity of animal samples prepandemic. What induces this cross-reactive response was not readily apparent. However, we propose several possibilities—exposure to another infectious agent generating cross-reactive antibodies, infection with multiple common coronavirus strains (feline coronavirus or otherwise) generating cross-reactive antibodies, or exposure of animals to a SARS-like coronavirus prepandemic.

There is evidence both for and against these explanations for the seropositivity observed. While we cannot discount a noncoronavirus infection generating cross-reactive antibodies, the RBD of SARS-like viruses is thought to be unique with no previous evidence of RBD cross-reactivity (32, 38, 46, 49). A plausible explanation for seropositivity against SARS-CoV-2's RBD is infections with coronaviruses generating an atypical response. To date, cross-reactivity against the RBD of SARS-CoV-2 has only been reported for SARS and SARS-like coronaviruses (32, 46). The common human and animal coronaviruses (both *Alpha-* and *Betacoronavirus* families) individually do not generate cross-reactive antibodies against this protein, presumably making it a SARS-specific response (30, 32, 33, 38, 46, 49). For example, prior FCoV exposure did not impact SARS-CoV-2 RBD recognition (38). Our own observations further demonstrated that FCoV (both serotype I and II) and transmissible gastroenteritis virus (TGEV) did not correlate with serostatus for SARS-CoV-2's RBD (Fig. 2A) (FCoV+, FCoV−). Additionally, humans and animals are exposed to multiple coronaviruses throughout their lifetime, generating measurable immune responses to antigenic proteins (69, 70). With humans, CoV infections occur on average once a year, with protective immunity appearing to wane a few months after initial exposure (69, 70). Despite reports of cross-reactivity toward portions of SARS-CoV-2's spike protein induced by other human coronaviruses, there have been no reports of cross-reaction against the distinct RBD region (32, 46, 49). While it does not disprove multiple CoV infections generating cross-reactive antibodies, it does cast doubt on this possibility. This leads us to propose prior exposure to a SARS-like coronavirus for North American cats.

There is limited evidence to support prior transmission of a SARS-like virus within felines. However, cats are susceptible to infection and transmission of SARS-CoV-2 (14). SARS coronaviruses evolved from bat coronaviruses and maintain a high degree of sequence similarity, even in the RBD region (32). Conceivably, our definition of SARS-like coronavirus could also encompass bat coronaviruses due to amino acid similarity and potential cross-reactivity in the RBD region. At least in Tennessee there are numerous cave systems with several native species of bats, potentially leading to an interspecies transmission. Feline and bat interactions could lead to direct transfer of a SARS-like agent, or an intermediary species could be involved. North American deer mice were recently shown to be susceptible to human SARS-CoV-2 and capable of mouse-to-mouse transmission, representing another potential point of introduction into the feline population (71). The prepandemic exposure of cats to a SARS-like agent does have detractions. Other groups examining prepandemic samples have failed to find evidence of RBD-reactive serum even within Central China (38, 56, 58). The ELISA-positive samples from our environmental samples (i.e., feline and deer) did not neutralize to the same degree as experimentally inoculated felines (Fig. 5B) (14). However, significant neutralization was not observed for most samples, even convalescent-phase serum from COVID-positive individuals (Fig. 5B). Despite ∼50% seroprevalence in our samples, we were unable to identify any coronavirus sequences capable of eliciting an anti-SARS RBD response (Fig. 6 and 7). Additionally, there is currently no evidence of a circulating SARS-like or bat betacoronavirus in North America (65–68). While we cannot conclusively demonstrate the origin of the anti-RBD responses shown here, this study indicates that there could be a virus (or another infectious agent) that can generate cross-reactive antibodies to the SARS-CoV-2 RBD.

Limitations of the study. A major limitation of this study is the number of serum samples surveyed for all species. Due to the small sample size, we have refrained from making extrapolations from our data to larger animal populations or geographic regions. Similarly, a relatively small number of feline fecal samples were screened for coronavirus viral RNA ($n = 30$), limiting our ability to detect coronaviruses. Our choice of sampling source may have also limited our ability to detect novel coronaviruses or SARS-like coronaviruses. We chose to utilize fecal samples for coronavirus screening because it is noninvasive, animal coronavirus shedding within feces is common, and many are transmitted via the fecal to oral route. Additionally, SARS-CoV and SARS-CoV-

2 viral RNA has been detected in stool samples of infected humans (8, 9, 11, 13). This fecally shed RNA persists longer than nasal or oral sources (13). However, sampling nasal/oral sources rather than fecal samples may allow for better detection of SARS-CoV-2. Indeed, isolation of SARS-CoV-2 RNA and whole-genome sequencing was possible from deer retropharyngeal lymph nodes (28). Along with sampling site limitations, infection and shedding of viral RNA is a transient process with a relatively small window to detect and sequence the causative agent. While ~20 feline samples were tested for anti-FCoV antibodies, the majority of our samples were of an unknown FCoV status. Additionally, medical histories were not available for these animals, and they were not screened for prior exposure to other infectious agents. As such, we cannot definitively rule out some other infectious agent conferring the anti-RBD responses.

Conclusion. Our initial goal was to develop an ELISA for tracking the reverse zoonosis of SARS-CoV-2. However, when establishing our baseline on prepandemic cat samples, we discovered seropositive serum for an antigen previously reported to be SARS-specific (i.e., RBD). Seropositivity was ~50% in feline samples and could be found several years prior to the genesis of the current SARS-CoV-2 pandemic. What generated the RBD-reactive antibodies is unknown, but we proposed three possibilities, cross-reaction caused by another infectious agent, multiple coronavirus infections creating a rare cross-reactive antibody, and existence and circulation of a SARS-related virus containing the RBD sequence. Regardless, the high rate of SARS-CoV-2 RBD seropositivity within a common companion animal further highlights our need for a better understanding of the prevalence and crossover potential of wild coronaviruses. Further investigations should address shedding of viral RNA from the seropositive species (i.e., cats and deer) identified here to isolate, sequence, and identify the agent enabling cross-reactivity against the RBD of SARS-CoV-2.

MATERIALS AND METHODS

Recombinant RBD production and purification. Recombinant RBD production has been previously published (56). Our lab deviated from the prior published method to utilize equipment readily available. Briefly, the plasmid containing the RBD of SARS-CoV-2 was produced under federal contract HHSN272201400008C and obtained through BEI Resources, NIAID, NIH. Vector pCAGGS contains the SARS-related coronavirus 2, Wuhan-Hu-1 spike glycoprotein RBD, NR-52309. To produce recombinant RBD, the pCAGGS-RBD plasmid was transfected into ~5 × 10^7 adherent HEK-293/T17 cells (ATCC CRL-11268) in a T-175 device using PEI (polyethylenimine, linear 25,000 molecular weight (m.w.) [Polysciences, Warrington, PA, USA]). Plasmid was mixed at a 1:3 ratio with PEI (20 μg of plasmid:60 μg PEI for a T-175 transfection) in 1 mL serum-free Dulbecco modified Eagle medium (DMEM) for 30 min at room temperature. Medium was aspirated, and the transfection mixture was added to 14 mL fresh growth medium and placed onto cells. Then, 3 to 4 h posttransfection, medium was changed and replaced with DMEM containing either 2% or 5% fetal bovine serum (HyClone FetalClone III; Cytiva Life Sciences, USA). Maintenance in a lower serum prevents overgrowth. However, we found higher protein yields with supplementation with 5% FBS. Transfection efficiency was nearly 100% as assessed by green fluorescent protein (GFP)-positive transfected cells in a control flask.

Supernatants from transfected HEK-293 T17 cells were collected into 50-mL conical tubes and frozen at days 3 and 6 posttransfection. Pooled supernatants were thawed and incubated with Ni-NTA (Ni-NTA agarose; Qiagen, Germany) resin with gentle rocking overnight. The resin was spun down at >3,400 × g in a swing-bucket Sorvall RT centrifuge for 10 min at 4°C. Ni-NTA resin was resuspended in 1 mL wash buffer (20 mM imidazole, 5 mM NaH$_2$PO$_4$·H$_2$O, and 0.3 M NaCl in H$_2$O), transferred to a 2-mL microcentrifuge tube, gently rocked for 10 min at room temperature, spun, and resuspended in fresh buffer. Resin was washed between 3 and 7 times until the OD$_{230}$ was ≤wash buffer. Once the supernatant OD dropped sufficiently, 1 mL elution buffer (235 mM imidazole, 5 mM NaH$_2$PO$_4$·H$_2$O, and 0.3 M NaCl in H$_2$O) was added to elute the RBD from the nickel resin. Eluate was rocked for 10 min at room temperature and then centrifuged. Two elution steps were performed with a third final elution using 0.5 M imidazole. Protein concentration was determined by standard curve analysis of a silver-stained (Pierce silver stain kit; Thermo Scientific, USA) 12% SDS-PAGE gel using a standard curve of BSA (bovine serum albumin). Analysis was performed using Image Studio Lite ver. 5.3 (Li-Cor Biosciences, Lincoln, NE, USA).

Serum and plasma samples. Previously collected pre-SARS-CoV-2 deidentified human serum samples were kindly donated by Jon Wall and Steve Foster (University of Tennessee Medical Center, Knoxville, TN, USA). Deidentified COVID-positive plasma samples were donated from MEDIC Regional Blood Center (Knoxville, TN, USA) and Mark Slifka (Oregon Health Sciences University, Portland, OR, USA). The following reagents were obtained through BEI Resources, NIAID, NIH: human plasma, sample IDs WU353-073, NR-53643; WU353-074, NR-53644; WU353-075, NR-53645; WU353-076, NR-53646; and WU353-076, NR-53647, were initially contributed by Ali Ellebedy, Washington University School of Medicine, St. Louis, MO, USA. The following reagents were obtained through BEI Resources, NIAID, NIH: polyclonal anti-feline infectious peritonitis virus, 79-1146 (antiserum, guinea pig), NR-2518; polyclonal anti-

canine coronavirus, UCD1 (antiserum, guinea pig), NR-2727; polyclonal anti-bovine coronavirus, Mebus (antiserum, guinea pig), NR-455; polyclonal anti-porcine respiratory coronavirus, ISU-1 (antiserum, guinea pig), NR-459; polyclonal anti-turkey coronavirus, Indiana (antiserum, guinea pig), NR-9465. Client-owned canine and feline serum samples were submitted to the University of Tennessee Veterinary Hospital for routine animal testing. Canine samples ($n = 36$) were collected postpandemic from local, East Tennessee animals. All feline samples were prepandemic. Samples from East Tennessee feral cats ($n = 36$) were collected from 2007 to 2012. Client-owned feline samples ($n = 92$) were collected nationwide as part of clinical diagnostic testing (see Table 1). Twenty cat samples were grouped into FCoV-positive and -negative groups based on feline infectious peritonitis (FIP) serology using an immunofluorescence assay (IFA) against FIP serotypes I and II, as well as TGEV (transmissible gastroenteritis virus) (VMRD, Pullman, WA, USA). Normal cat serum was purchased from Jackson ImmunoResearch (West Grove, PA, USA). Tennessee-resident cows ($n = 33$) and tigers ($n = 9$) were collected prepandemic for routine diagnostic testing. Postmortem, postpandemic samples were collected from East Tennessee elk ($n = 12$) and South Carolina white-tailed deer ($n = 22$).

Anti-RBD ELISA. Anti-RBD ELISA was based on the published protocol by Amanat et al. and Stadlbauer et al. (30, 59). Purified RBD was diluted to 2 μg/mL in phosphate-buffered saline (PBS), and 50 μL was placed into each well of a 96-well plate (Immulon 4HBX, Thermo Fisher, USA) and allowed to incubate overnight at 4°C. Unbound RBD was removed, and wells were washed 3 times with PBS-T (PBS with 0.1% Tween 20). Rinsed wells were blocked with 5% milk in PBS for 2 h at room temperature. Block was removed and serum or plasma samples were added at a 1:50 dilution for the initial screen in PBS with 1% milk and incubated at room temperature for 1 h. After 1 h, wells were washed 3 times with PBS-T, and a secondary antibody for that species was added (i.e., horseradish peroxidase [HRP] goat anti-human IgG, Rockland Immunochemicals, Pottstown, PA, USA; HRP goat anti-dog IgG, Bethyl Laboratories, Montgomery, TX, USA; HRP goat anti-cat IgG, Invitrogen, Waltham, MA, USA; HRP goat anti-guinea pig IgG, Life Technologies Corp., Carlsbad, CA, USA; HRP rabbit anti-deer IgG, KPL, Gaithersburg, MD, USA; HRP sheep anti-cow IgG, Bethyl Laboratories, Montgomery, TX, USA) at dilutions of 1:10,000 (anti-human, -cat, -dog, -tiger) or 1:250 (anti-cow, -deer, -elk) in PBS with 1% milk. Optimal secondary antibody concentrations were determined by titration on either 5% milk (negative control) or a 1:50 dilution of that species serum (positive control). Secondary antibodies were allowed to incubate for 1 h at room temperature before being washed 3 times with PBS-T. ELISA was developed with 50 μL TMB (1-Step Ultra TMB-ELISA; Thermo Fisher, Waltham, MA, USA) for 10 min. Reactions were stopped by the addition of 2 M sulfuric acid and read using a BioTek Synergy 2 or Synergy H1 plate reader set at 450 nm (BioTek, Winooski, VT, USA). Receiver operator curve (ROC) analysis was performed to determine the appropriate threshold to yield 100% specificity of ELISAs performed at a 1:50 dilution. For titrations of seropositive and seronegative samples, threshold values for each dilution were calculated as the average of negative samples plus 3 times the standard deviation. Titrated samples were initially diluted 1:100 and then serially diluted 1:3 (final dilution of 1:8,100). Serum dilutions were made in PBS with 1% milk and added to RBD-coated and blocked wells. OD_{450} values for each species and titrations were graphed in Prism ver. 8 (GraphPad Software, San Diego, CA, USA).

Western and dot blots. For dot blots, 5 to 10 μL of sample was applied directly onto nitrocellulose membranes and allowed to dry. Western blots were loaded with 30 μL ($\sim$3 μg) of purified recombinant RBD, resolved in a 12% SDS-PAGE gel, and transferred to a nitrocellulose membrane. Blots were blocked overnight at 4°C with 5% milk in PBS. Mouse anti-6×His-HRP conjugated antibody (1:5,000) (Proteintech, Rosemont, IL, USA) or polyclonal serum samples (1:20) were incubated with the blots at room temperature for 2 h and subsequently washed 2 times with TBS-T (tris buffered saline with 0.1% Tween 20). For polyclonal serum, species-specific HRP anti-IgG antibodies (1:5,000 dilution) were incubated for an additional 2 h and washed 2 times as described above. Chemiluminescent substrate (Pierce SuperSignal West Pico PLUS; Thermo Fisher, USA) was added, and luminescence was detected using ChemiDoc (Bio-Rad, Hercules, CA, USA).

Neutralization assays. Serum samples were screened for neutralization using LEGENDplex SARS-CoV-2 neutralizing antibody assay (BioLegend, San Diego, CA, USA) following the manufacturer's recommendations. Briefly, serum was diluted 1:100 and incubated with biotinylated SARS-CoV-2 S1 subunit containing the RBD and human ACE-2 (hACE-2) conjugated to fluorescent beads. Streptavidin-PE (phycoerythrin) was added to detect SARS-CoV-2 S1 subunit bound to beads/hACE-2. Binding/PE levels were detected via a BD LSR-II instrument equipped with 488- and 633-nm lasers (Becton, Dickinson, Franklin Lakes, NJ, USA). Data were analyzed using BioLegend LEGENDplex data analysis software. Mean fluorescent intensity (MFI) was normalized and graphed in Prism ver. 9 (GraphPad Software, San Diego, CA, USA).

Fecal coronavirus PCR screen and sequence alignments. Deidentified fecal samples from 30 healthy East Tennessee cats were collected and stored at −80°C. Samples were resuspended in PBS to yield a 10% solution and centrifuged to clarify. Fecal RNA was extracted using a viral RNA extraction kit (Qiagen, Hilden, Germany), and RNA was reverse transcribed using a Verso cDNA kit with random hexamers and RT enhancer (Thermo Fisher, Waltham, MA, USA). PCR amplification of conserved coronavirus regions using previously reported primer pairs was used to screen the cDNA (62). PCR amplicons were visualized on a 1% agarose gel, and positive PCR samples were Sanger dideoxy sequenced. Sequences were viewed using 4Peaks software (Nucleobytes, Amsterdam, Netherlands). Sequences from fecal samples were Clustal W aligned to common coronaviruses and trimmed, and phylogenetic trees were generated using the maximum-likelihood method for each positive loci using MEGA X (72, 73). For phylogenetic trees using multiple loci, aligned and trimmed sequences for each loci were concatenated together prior to maximum-likelihood tree construction. Phylogenetic trees were tested by bootstrap testing with 1,000 iterations. Common coronavirus sequences for ORF1ab (RdRp and helicase loci) and spike were obtained from the following: porcine coronavirus HKU15 (GenBank accession number NC039208),

SARS-CoV-2 (MN988668), SARS-CoV (NC004718), porcine respiratory coronavirus/PRCoV (KY406735), human coronavirus OC43 (NC006213), MERS-CoV (NC038294), feline coronavirus/FCoV (NC002306), canine respiratory coronavirus/CRCoV (KX432213), canine coronavirus/CCoV (JQ404410), bovine coronavirus/BCoV (NC003045), avian coronavirus (NC048214), human coronavirus 229E (NC002645), transmissible gastroenteritis virus/TGEV (NC038861), murine hepatitis virus/MHV (NC048217), human coronavirus NL63 (NC005831), feline coronavirus strain UU8 (FJ938055), feline coronavirus strain UU19 (HQ392470), feline coronavirus strain Black (EU186072), feline coronavirus strain RM (FJ938051), and feline coronavirus strain Felix (MG893511).

Data availability. All generated sequences were deposited in GenBank under accession numbers MZ220722 through MZ220762 (sample ID, positive loci, animal location, and accession numbers are shown in Table 2). Data are available upon request for peer review.

Statistics. All graphs and statistical analyses were performed in Prism ver. 9 (GraphPad Software, San Diego, CA, USA). ELISA OD_{450} results were normalized to an interplate replicate run with all assays. Student's one-tailed t tests with Welch's correction and one-way analysis of variance (ANOVA) with multiple-comparison tests were performed on ELISA results and documented in the figure legends. Descriptive statistics were provided for each ELISA group (mean, median, and quartiles). Receiver operator curve (ROC) analysis was performed to determine appropriate threshold values for human, cat, and deer serum samples. The area under the curve was calculated for each titrated ELISA sample and graphed. Neutralization data were normalized with the negative-control group (normal cat serum) representing 100% MFI.

REFERENCES

1. Poon LLM, Peiris M. 2020. Emergence of a novel human coronavirus threatening human health. Nat Med 26:317–319. https://doi.org/10.1038/s41591-020-0796-5.

2. Guan W-J, Ni Z-Y, Hu Y, Liang W-H, Ou C-Q, He J-X, Liu L, Shan H, Lei C-L, Hui DSC, Du B, Li L-J, Zeng G, Yuen K-Y, Chen R-C, Tang C-L, Wang T, Chen P-Y, Xiang J, Li S-Y, Wang J-L, Liang Z-J, Peng Y-X, Wei L, Liu Y, Hu Y-H, Peng P, Wang J-M, Liu J-Y, Chen Z, Li G, Zheng Z-J, Qiu S-Q, Luo J, Ye C-J, Zhu S-Y, Zhong N-S, China Medical Treatment Expert Group for Covid-19. 2020. Clinical characteristics of coronavirus disease 2019 in China. N Engl J Med 382:1708–1720. https://doi.org/10.1056/NEJMoa2002032.

3. Latinne A, Hu B, Olival KJ, Zhu G, Zhang L, Li H, Chmura AA, Field HE, Zambrana-Torrelio C, Epstein JH, Li B, Zhang W, Wang L-F, Shi Z-L, Daszak P. 2020. Origin and cross-species transmission of bat coronaviruses in China. Nat Commun 11:4235. https://doi.org/10.1038/s41467-020-17687-3.

4. Li X, Giorgi EE, Marichannegowda MH, Foley B, Xiao C, Kong X-P, Chen Y, Gnanakaran S, Korber B, Gao F. 2020. Emergence of SARS-CoV-2 through recombination and strong purifying selection. Sci Adv 6:eabb9153. https://doi.org/10.1126/sciadv.abb9153.

5. Andersen KG, Rambaut A, Lipkin WI, Holmes EC, Garry RF. 2020. The proximal origin of SARS-CoV-2. Nat Med 26:450–452. https://doi.org/10.1038/s41591-020-0820-9.

6. Sun J, Xiao J, Sun R, Tang X, Liang C, Lin H, Zeng L, Hu J, Yuan R, Zhou P, Peng J, Xiong Q, Cui F, Liu Z, Lu J, Tian J, Ma W, Ke C. 2020. Prolonged persistence of SARS-CoV-2 RNA in body fluids. Emerg Infect Dis 26:1834–1838. https://doi.org/10.3201/eid2608.201097.

7. Meyerowitz EA, Richterman A, Gandhi RT, Sax PE. 2021. Transmission of SARS-CoV-2: a review of viral, host, and environmental factors. Ann Intern Med 174:69–79. https://doi.org/10.7326/M20-5008.

8. Wang W, Xu Y, Gao R, Lu R, Han K, Wu G, Tan W. 2020. Detection of SARS-CoV-2 in different types of clinical specimens. JAMA 323:1843–1844. https://doi.org/10.1001/jama.2020.3786.

9. Kim J-M, Kim HM, Lee EJ, Jo HJ, Yoon Y, Lee N-J, Son J, Lee Y-J, Kim MS, Lee Y-P, Chae S-J, Park KR, Cho S-R, Park S, Kim SJ, Wang E, Woo SH, Lim A, Park S-J, Jang J, Chung Y-S, Chin BS, Lee J-S, Lim D, Han M-G, Yoo CK. 2020. Detection and isolation of SARS-CoV-2 in serum, urine, and stool specimens of COVID-19 patients from the Republic of Korea. Osong Public Health Res Perspect 11:112–117. https://doi.org/10.24171/j.phrp.2020.11.3.02.

10. Kang M, Wei J, Yuan J, Guo J, Zhang Y, Hang J, Qu Y, Qian H, Zhuang Y, Chen X, Peng X, Shi T, Wang J, Wu J, Song T, He J, Li Y, Zhong N. 2020. Probable evidence of fecal aerosol transmission of SARS-CoV-2 in a high-rise building. Ann Intern Med 173:974–980. https://doi.org/10.7326/M20-0928.

11. Xiao F, Sun J, Xu Y, Li F, Huang X, Li H, Zhao J, Huang J, Zhao J. 2020. Infectious SARS-CoV-2 in feces of patient with severe COVID-19. Emerg Infect Dis 26:1920–1922. https://doi.org/10.3201/eid2608.200681.

12. Yu ITS, Li Y, Wong TW, Tam W, Chan AT, Lee JHW, Leung DYC, Ho T. 2004. Evidence of airborne transmission of the severe acute respiratory syndrome virus. N Engl J Med 350:1731–1739. https://doi.org/10.1056/NEJMoa032867.

13. Roltgen K, Powell AE, Wirz OF, Stevens BA, Hogan CA, Najeeb J, Hunter M, Wang H, Sahoo MK, Huang C, Yamamoto F, Manohar M, Manalac J, Otrelo-Cardoso AR, Pham TD, Rustagi A, Rogers AJ, Shah NH, Blish CA, Cochran JR, Jardetzky TS, Zehnder JL, Wang TT, Narasimhan B, Gombar S, Tibshirani R, Nadeau KC, Kim PS, Pinsky BA, Boyd SD. 2020. Defining the features and duration of antibody responses to SARS-CoV-2 infection associated with disease severity and outcome. Sci Immunol 5:eabe0240. https://doi.org/10.1126/sciimmunol.abe0240.

14. Bosco-Lauth AM, Hartwig AE, Porter SM, Gordy PW, Nehring M, Byas AD, VandeWoude S, Ragan IK, Maison RM, Bowen RA. 2020. Experimental infection of domestic dogs and cats with SARS-CoV-2: pathogenesis, transmission, and response to reexposure in cats. Proc Natl Acad Sci U S A 117:26382–26388. https://doi.org/10.1073/pnas.2013102117.

15. Shi J, Wen Z, Zhong G, Yang H, Wang C, Huang B, Liu R, He X, Shuai L, Sun Z, Zhao Y, Liu P, Liang L, Cui P, Wang J, Zhang X, Guan Y, Tan W, Wu G, Chen H, Bu Z. 2020. Susceptibility of ferrets, cats, dogs, and other domesticated animals to SARS-coronavirus 2. Science 368:1016–1020. https://doi.org/10.1126/science.abb7015.

16. Wu L, Chen Q, Liu K, Wang J, Han P, Zhang Y, Hu Y, Meng Y, Pan X, Qiao C, Tian S, Du P, Song H, Shi W, Qi J, Wang H-W, Yan J, Gao GF, Wang Q. 2020. Broad host range of SARS-CoV-2 and the molecular basis for SARS-CoV-2 binding to cat ACE2. Cell Discov 6:68. https://doi.org/10.1038/s41421-020-00210-9.

17. Segales J, Puig M, Rodon J, Avila-Nieto C, Carrillo J, Cantero G, Terrón MT, Cruz S, Parera M, Noguera-Julián M, Izquierdo-Useros N, Guallar V, Vidal E, Valencia A, Blanco I, Blanco J, Clotet B, Vergara-Alert J. 2020. Detection of

SARS-CoV-2 in a cat owned by a COVID-19-affected patient in Spain. Proc Natl Acad Sci U S A 117:24790–24793. https://doi.org/10.1073/pnas.2010817117.

18. Fritz M, Rosolen B, Krafft E, Becquart P, Elguero E, Vratskikh O, Denolly S, Boson B, Vanhomwegen J, Gouilh MA, Kodjo A, Chirouze C, Rosolen SG, Legros V, Leroy EM. 2021. High prevalence of SARS-CoV-2 antibodies in pets from COVID-19+ households. One Health 11:100192.

19. Sit THC, Brackman CJ, Ip SM, Tam KWS, Law PYT, To EMW, Yu VYT, Sims LD, Tsang DNC, Chu DKW, Perera RAPM, Poon LLM, Peiris M. 2020. Infection of dogs with SARS-CoV-2. Nature 586:776–778. https://doi.org/10.1038/s41586-020-2334-5.

20. Patterson EI, Elia G, Grassi A, Giordano A, Desario C, Medardo M, Smith SL, Anderson ER, Prince T, Patterson GT, Lorusso E, Lucente MS, Lanave G, Lauzi S, Bonfanti U, Stranieri A, Martella V, Solari Basano F, Barrs VR, Radford AD, Agrimi U, Hughes GL, Paltrinieri S, Decaro N. 2020. Evidence of exposure to SARS-CoV-2 in cats and dogs from households in Italy. Nat Commun 11:6231. https://doi.org/10.1038/s41467-020-20097-0.

21. Barrs VR, Peiris M, Tam KWS, Law PYT, Brackman CJ, To EMW, Yu VYT, Chu DKW, Perera RAPM, Sit THC. 2020. SARS-CoV-2 in quarantine domestic cats from COVID-19 households or close contacts, Hong Kong, China. Emerg Infect Dis 26:3071–3074. https://doi.org/10.3201/eid2612.202786.

22. Halfmann PJ, Hatta M, Chiba S, Maemura T, Fan S, Takeda M, Kinoshita N, Hattori S-I, Sakai-Tagawa Y, Iwatsuki-Horimoto K, Imai M, Kawaoka Y. 2020. Transmission of SARS-CoV-2 in domestic cats. N Engl J Med 383:592–594. https://doi.org/10.1056/NEJMc2013400.

23. Oude Munnink BB, Sikkema RS, Nieuwenhuijse DF, Molenaar RJ, Munger E, Molenkamp R, van der Spek A, Tolsma P, Rietveld A, Brouwer M, Bouwmeester-Vincken N, Harders F, Hakze-van der Honing R, Wegdam-Blans MCA, Bouwstra RJ, GeurtsvanKessel C, van der Eijk AA, Velkers FC, Smit LAM, Stegeman A, van der Poel WHM, Koopmans MPG. 2021. Transmission of SARS-CoV-2 on mink farms between humans and mink and back to humans. Science 371:172–177. https://doi.org/10.1126/science.abe5901.

24. Martina BEE, Haagmans BL, Kuiken T, Fouchier RAM, Rimmelzwaan GF, Van Amerongen G, Peiris JSM, Lim W, Osterhaus ADME. 2003. Virology: SARS virus infection of cats and ferrets. Nature 425:915. https://doi.org/10.1038/425915a.

25. Ng SK. 2003. Possible role of an animal vector in the SARS outbreak at Amoy Gardens. Lancet 362:570–572. https://doi.org/10.1016/S0140-6736(03)14121-9.

26. Lun ZR, Qu LH. 2004. Animal-to-human SARS-associated coronavirus transmission? Emerg Infect Dis 10:959. https://doi.org/10.3201/eid1005.040022.

27. Hale VL, Dennis PM, McBride DS, Nolting JM, Madden C, Huey D, Ehrlich M, Grieser J, Winston J, Lombardi D, Gibson S, Saif L, Killian ML, Lantz K, Tell RM, Torchetti M, Robbe-Austerman S, Nelson MI, Faith SA, Bowman AS. 2022. SARS-CoV-2 infection in free-ranging white-tailed deer. Nature 602:481–486. https://doi.org/10.1038/s41586-021-04353-x.

28. Kuchipudi SV, Surendran-Nair M, Ruden RM, Yon M, Nissly RH, Vandegrift KJ, Nelli RK, Li L, Jayarao BM, Maranas CD, Levine N, Willgert K, Conlan AJK, Olsen RJ, Davis JJ, Musser JM, Hudson PJ, Kapur V. 2022. Multiple spillovers from humans and onward transmission of SARS-CoV-2 in white-tailed deer. Proc Natl Acad Sci U S A 119:e2121644119. https://doi.org/10.1073/pnas.2121644119.

29. Chandler JC, Bevins SN, Ellis JW, Linder TJ, Tell RM, Jenkins-Moore M, Root JJ, Lenoch JB, Robbe-Austerman S, DeLiberto TJ, Gidlewski T, Torchetti MK, Shriner SA. 2021. SARS-CoV-2 exposure in wild white-tailed deer (Odocoileus virginianus). Proc Natl Acad Sci U S A 118:e2114828118. https://doi.org/10.1073/pnas.2114828118.

30. Amanat F, Stadlbauer D, Strohmeier S, Nguyen THO, Chromikova V, McMahon M, Jiang K, Arunkumar GA, Jurczyszak D, Polanco J, Bermudez-Gonzalez M, Kleiner G, Aydillo T, Miorin L, Fierer DS, Lugo LA, Kojic EM, Stoever J, Liu STH, Cunningham-Rundles C, Felgner PL, Moran T, García-Sastre A, Caplivski D, Cheng AC, Kedzierska K, Vapalahti O, Hepojoki JM, Simon V, Krammer F. 2020. A serological assay to detect SARS-CoV-2 seroconversion in humans. Nat Med 26:1033–1036. https://doi.org/10.1038/s41591-020-0913-5.

31. Long Q-X, Liu B-Z, Deng H-J, Wu G-C, Deng K, Chen Y-K, Liao P, Qiu J-F, Lin Y, Cai X-F, Wang D-Q, Hu Y, Ren J-H, Tang N, Xu Y-Y, Yu L-H, Mo Z, Gong F, Zhang X-L, Tian W-G, Hu L, Zhang X-X, Xiang J-L, Du H-X, Liu H-W, Lang C-H, Luo X-H, Wu S-B, Cui X-P, Zhou Z, Zhu M-M, Wang J, Xue C-J, Li X-F, Wang L, Li Z-J, Wang K, Niu C-C, Yang Q-J, Tang X-J, Zhang Y, Liu X-M, Li J-J, Zhang D-C, Zhang F, Liu P, Yuan J, Li Q, Hu J-L, Chen J, et al. 2020. Antibody responses to SARS-CoV-2 in patients with COVID-19. Nat Med 26:845–848., https://doi.org/10.1038/s41591-020-0897-1.

32. Premkumar L, Segovia-Chumbez B, Jadi R, Martinez DR, Raut R, Markmann A, Cornaby C, Bartelt L, Weiss S, Park Y, Edwards CE, Weimer E, Scherer EM, Rouphael N, Edupuganti S, Weiskopf D, Tse LV, Hou YJ, Margolis D, Sette A, Collins MH, Schmitz J, Baric RS, de Silva AM. 2020. The receptor binding domain of the viral spike protein is an immunodominant and highly specific target of antibodies in SARS-CoV-2 patients. Sci Immunol 5:eabc8413. https://doi.org/10.1126/sciimmunol.abc8413.

33. Suthar MS, Zimmerman MG, Kauffman RC, Mantus G, Linderman SL, Hudson WH, Vanderheiden A, Nyhoff L, Davis CW, Adekunle O, Affer M, Sherman M, Reynolds S, Verkerke HP, Alter DN, Guarner J, Bryksin J, Horwath MC, Arthur CM, Saakadze N, Smith GH, Edupuganti S, Scherer EM, Hellmeister K, Cheng A, Morales JA, Neish AS, Stowell SR, Frank F, Ortlund E, Anderson EJ, Menachery VD, Rouphael N, Mehta AK, Stephens DS, Ahmed R, Roback JD, Wrammert J. 2020. Rapid generation of neutralizing antibody responses in COVID-19 patients. Cell Rep Med 1:100040. https://doi.org/10.1016/j.xcrm.2020.100040.

34. Desmarets LMB, Vermeulen BL, Theuns S, Conceição-Neto N, Zeller M, Roukaerts IDM, Acar DD, Olyslaegers DAJ, Van Ranst M, Matthijnssens J, Nauwynck HJ. 2016. Experimental feline enteric coronavirus infection reveals an aberrant infection pattern and shedding of mutants with impaired infectivity in enterocyte cultures. Sci Rep 6:20022. https://doi.org/10.1038/srep20022.

35. Vogel L, Van der Lubben M, Te Lintelo EG, Bekker CPJ, Geerts T, Schuijff LS, Grinwis GCM, Egberink HF, Rottier PJM. 2010. Pathogenic characteristics of persistent feline enteric coronavirus infection in cats. Vet Res 41:71. https://doi.org/10.1051/vetres/2010043.

36. Cevik M, Tate M, Lloyd O, Maraolo AE, Schafers J, Ho A. 2021. SARS-CoV-2, SARS-CoV, and MERS-CoV viral load dynamics, duration of viral shedding, and infectiousness: a systematic review and meta-analysis. Lancet Microbe 2:e13–e22. https://doi.org/10.1016/S2666-5247(20)30172-5.

37. Addie DD, Jarrett O. 2001. Use of a reverse-transcriptase polymerase chain reaction for monitoring the shedding of feline coronavirus by healthy cats. Vet Rec 148:649–653. https://doi.org/10.1136/vr.148.21.649.

38. Zhang Q, Zhang H, Gao J, Huang K, Yang Y, Hui X, He X, Li C, Gong W, Zhang Y, Zhao Y, Peng C, Gao X, Chen H, Zou Z, Shi Z-L, Jin M. 2020. A serological survey of SARS-CoV-2 in cat in Wuhan. Emerg Microbes Infect 9:2013–2019. https://doi.org/10.1080/22221751.2020.1817796.

39. Liu W, Fontanet A, Zhang P-H, Zhan L, Xin Z-T, Baril L, Tang F, Lv H, Cao W-C. 2006. Two-year prospective study of the humoral immune response of patients with severe acute respiratory syndrome. J Infect Dis 193:792–795. https://doi.org/10.1086/500469.

40. Cao W-C, Liu W, Zhang P-H, Zhang F, Richardus JH. 2007. Disappearance of antibodies to SARS-associated coronavirus after recovery. N Engl J Med 357:1162–1163. https://doi.org/10.1056/NEJMc070348.

41. Lin Q, Zhu L, Ni Z, Meng H, You L. 2020. Duration of serum neutralizing antibodies for SARS-CoV-2: lessons from SARS-CoV infection. J Microbiol Immunol Infect 53:821–822. https://doi.org/10.1016/j.jmii.2020.03.015.

42. Tang F, Quan Y, Xin Z-T, Wrammert J, Ma M-J, Lv H, Wang T-B, Yang H, Richardus JH, Liu W, Cao W-C. 2011. Lack of peripheral memory B cell responses in recovered patients with severe acute respiratory syndrome: a six-year follow-up study. J Immunol 186:7264–7268. https://doi.org/10.4049/jimmunol.0903490.

43. Zeng W, Liu G, Ma H, Zhao D, Yang Y, Liu M, Mohammed A, Zhao C, Yang Y, Xie J, Ding C, Ma X, Weng J, Gao Y, He H, Jin T. 2020. Biochemical characterization of SARS-CoV-2 nucleocapsid protein. Biochem Biophys Res Commun 527:618–623. https://doi.org/10.1016/j.bbrc.2020.04.136.

44. Hoffmann M, Kleine-Weber H, Schroeder S, Krüger N, Herrler T, Erichsen S, Schiergens TS, Herrler G, Wu N-H, Nitsche A, Müller MA, Drosten C, Pöhlmann S. 2020. SARS-CoV-2 cell entry depends on ACE2 and TMPRSS2 and is blocked by a clinically proven protease inhibitor. Cell 181:271–280.e8. https://doi.org/10.1016/j.cell.2020.02.052.

45. Lan J, Ge J, Yu J, Shan S, Zhou H, Fan S, Zhang Q, Shi X, Wang Q, Zhang L, Wang X. 2020. Structure of the SARS-CoV-2 spike receptor-binding domain bound to the ACE2 receptor. Nature 581:215–220. https://doi.org/10.1038/s41586-020-2180-5.

46. Ng KW, Faulkner N, Cornish GH, Rosa A, Harvey R, Hussain S, Ulferts R, Earl C, Wrobel AG, Benton DJ, Roustan C, Bolland W, Thompson R, Agua-Doce A, Hobson P, Heaney J, Rickman H, Paraskevopoulou S, Houlihan CF, Thomson K, Sanchez E, Shin GY, Spyer MJ, Joshi D, O'Reilly N, Walker PA, Kjaer S, Riddell A, Moore C, Jebson BR, Wilkinson M, Marshall LR, Rosser EC, Radziszewska A, Peckham H, Ciurtin C, Wedderburn LR, Beale R, Swanton C, Gandhi S, Stockinger B, McCauley J, Gamblin SJ, McCoy LE, Cherepanov P, Nastouli E, Kassiotis G. 2020. Preexisting and de novo

humoral immunity to SARS-CoV-2 in humans. Science 370:1339–1343. https://doi.org/10.1126/science.abe1107.

47. Chi X, Yan R, Zhang J, Zhang G, Zhang Y, Hao M, Zhang Z, Fan P, Dong Y, Yang Y, Chen Z, Guo Y, Zhang J, Li Y, Song X, Chen Y, Xia L, Fu L, Hou L, Xu J, Yu C, Li J, Zhou Q, Chen W. 2020. A neutralizing human antibody binds to the N-terminal domain of the Spike protein of SARS-CoV-2. Science 369:650–655. https://doi.org/10.1126/science.abc6952.

48. Song G, He W-T, Callaghan S, Anzanello F, Huang D, Ricketts J, Torres JL, Beutler N, Peng L, Vargas S, Cassell J, Parren M, Yang L, Ignacio C, Smith DM, Voss JE, Nemazee D, Ward AB, Rogers T, Burton DR, Andrabi R. 2021. Cross-reactive serum and memory B-cell responses to spike protein in SARS-CoV-2 and endemic coronavirus infection. Nat Commun 12:2938. https://doi.org/10.1038/s41467-021-23074-3.

49. Anderson EM, Goodwin EC, Verma A, Arevalo CP, Bolton MJ, Weirick ME, Gouma S, McAllister CM, Christensen SR, Weaver J, Hicks P, Manzoni TB, Oniyide O, Ramage H, Mathew D, Baxter AE, Oldridge DA, Greenplate AR, Wu JE, Alanio C, D'Andrea K, Kuthuru O, Dougherty J, Pattekar A, Kim J, Han N, Apostolidis SA, Huang AC, Vella LA, Kuri-Cervantes L, Pampena MB, Betts MR, Wherry EJ, Meyer NJ, Cherry S, Bates P, Rader DJ, Hensley SE. 2021. Seasonal human coronavirus antibodies are boosted upon SARS-CoV-2 infection but not associated with protection. Cell 184:1858–1864.e10. https://doi.org/10.1016/j.cell.2021.02.010.

50. Lee WT, Girardin RC, Dupuis AP, Kulas KE, Payne AF, Wong SJ, Arinsburg S, Nguyen FT, Mendu DR, Firpo-Betancourt A, Jhang J, Wajnberg A, Krammer F, Cordon-Cardo C, Amler S, Montecalvo M, Hutton B, Taylor J, McDonough KA. 2021. Neutralizing antibody responses in COVID-19 convalescent sera. J Infect Dis 223:47–55. https://doi.org/10.1093/infdis/jiaa673.

51. Rogers TF, Zhao F, Huang D, Beutler N, Burns A, He W-T, Limbo O, Smith C, Song G, Woehl J, Yang L, Abbott RK, Callaghan S, Garcia E, Hurtado J, Parren M, Peng L, Ramirez S, Ricketts J, Ricciardi MJ, Rawlings SA, Wu NC, Yuan M, Smith DM, Nemazee D, Teijaro JR, Voss JE, Wilson IA, Andrabi R, Briney B, Landais E, Sok D, Jardine JG, Burton DR. 2020. Isolation of potent SARS-CoV-2 neutralizing antibodies and protection from disease in a small animal model. Science 369:956–963. https://doi.org/10.1126/science.abc7520.

52. Niu L, Wittrock KN, Clabaugh GC, Srivastava V, Cho MW. 2021. A structural landscape of neutralizing antibodies against SARS-CoV-2 receptor binding domain. Front Immunol 12:647934. https://doi.org/10.3389/fimmu.2021.647934.

53. Zhou Y, Liu Z, Li S, Xu W, Zhang Q, Silva IT, Li C, Wu Y, Jiang Q, Liu Z, Wang Q, Guo Y, Wu J, Gu C, Cai X, Qu D, Mayer CT, Wang X, Jiang S, Ying T, Yuan Z, Xie Y, Wen Y, Lu L, Wang Q. 2021. Enhancement versus neutralization by SARS-CoV-2 antibodies from a convalescent donor associates with distinct epitopes on the RBD. Cell Rep 34:108699. https://doi.org/10.1016/j.celrep.2021.108699.

54. Zhu Y, Yu D, Han Y, Yan H, Chong H, Ren L, Wang J, Li T, He Y. 2020. Cross-reactive neutralization of SARS-CoV-2 by serum antibodies from recovered SARS patients and immunized animals. Sci Adv 6:eabc9999. https://doi.org/10.1126/sciadv.abc9999.

55. Lv H, Wu NC, Tsang OT-Y, Yuan M, Perera RAPM, Leung WS, So RTY, Chan JMC, Yip GK, Chik TSH, Wang Y, Choi CYC, Lin Y, Ng WW, Zhao J, Poon LLM, Peiris JSM, Wilson IA, Mok CKP. 2020. Cross-reactive antibody response between SARS-CoV-2 and SARS-CoV infections. Cell Rep 31:107725. https://doi.org/10.1016/j.celrep.2020.107725.

56. Zhao S, Li W, Schuurman N, van Kuppeveld F, Bosch B-J, Egberink H. 2019. Serological screening for coronavirus infections in cats. Viruses 11:743. https://doi.org/10.3390/v11080743.

57. Deng J, Jin Y, Liu Y, Sun J, Hao L, Bai J, Huang T, Lin D, Jin Y, Tian K. 2020. Serological survey of SARS-CoV-2 for experimental, domestic companion and wild animals excludes intermediate hosts of 35 different species of animals. Transbound Emerg Dis 67:1745–1749. https://doi.org/10.1111/tbed.13577.

58. Deng J, Liu Y, Sun C, Bai J, Sun J, Hao L, Li X, Tian K. 2020. SARS-CoV-2 serological survey of cats in China before and after the pandemic. Virol Sin 35:846–848. https://doi.org/10.1007/s12250-020-00284-1.

59. Stadlbauer D, Amanat F, Chromikova V, Jiang K, Strohmeier S, Arunkumar GA, Tan J, Bhavsar D, Capuano C, Kirkpatrick E, Meade P, Brito RN, Teo C,

60. Johari YB, Jaffé SRP, Scarrott JM, Johnson AO, Mozzanino T, Pohle TH, Maisuria S, Bhayat-Cammack A, Lambiase G, Brown AJ, Tee KL, Jackson PJ, Wong TS, Dickman MJ, Sargur RB, James DC. 2021. Production of trimeric SARS-CoV-2 spike protein by CHO cells for serological COVID-19 testing. Biotechnol Bioeng 118:1013–1021. https://doi.org/10.1002/bit.27615.

61. Palmer MV, Martins M, Falkenberg S, Buckley A, Caserta LC, Mitchell PK, Cassmann ED, Rollins A, Zylich NC, Renshaw RW, Guarino C, Wagner B, Lager K, Diel DG. 2021. Susceptibility of white-tailed deer (Odocoileus virginianus) to SARS-CoV-2. J Virol 95. https://doi.org/10.1128/JVI.00083-21.

62. Poon LLM, Chu DKW, Chan KH, Wong OK, Ellis TM, Leung YHC, Lau SKP, Woo PCY, Suen KY, Yuen KY, Guan Y, Peiris JSM. 2005. Identification of a novel coronavirus in bats. J Virol 79:2001–2009. https://doi.org/10.1128/JVI.79.4.2001-2009.2005.

63. Rattanapisit K, Shanmugaraj B, Manopwisedjaroen S, Purwono PB, Siriwattananon K, Khorattanakulchai N, Hanittinan O, Boonyayothin W, Thitithanyanont A, Smith DR, Phoolcharoen W. 2020. Rapid production of SARS-CoV-2 receptor binding domain (RBD) and spike specific monoclonal antibody CR3022 in Nicotiana benthamiana. Sci Rep 10:17698. https://doi.org/10.1038/s41598-020-74904-1.

64. Xiaojie S, Yu L, Lei Y, Guang Y, Min Q. 2020. Neutralizing antibodies targeting SARS-CoV-2 spike protein. Stem Cell Res 50:102125.

65. Olival KJ, Cryan PM, Amman BR, Baric RS, Blehert DS, Brook CE, Calisher CH, Castle KT, Coleman JTH, Daszak P, Epstein JH, Field H, Frick WF, Gilbert AT, Hayman DTS, Ip HS, Karesh WB, Johnson CK, Kading RC, Kingston T, Lorch JM, Mendenhall IH, Peel AJ, Phelps KL, Plowright RK, Reeder DM, Reichard JD, Sleeman JM, Streicker DG, Towner JS, Wang L-F. 2020. Possibility for reverse zoonotic transmission of SARS-CoV-2 to free-ranging wildlife: a case study of bats. PLoS Pathog 16:e1008758. https://doi.org/10.1371/journal.ppat.1008758.

66. Dominguez SR, O'Shea TJ, Oko LM, Holmes KV. 2007. Detection of group 1 coronaviruses in bats in North America. Emerg Infect Dis 13:1295–1300. https://doi.org/10.3201/eid1309.070491.

67. Misra V, Dumonceaux T, Dubois J, Willis C, Nadin-Davis S, Severini A, Wandeler A, Lindsay R, Artsob H. 2009. Detection of polyoma and corona viruses in bats of Canada. J Gen Virol 90:2015–2022. https://doi.org/10.1099/vir.0.010694-0.

68. Osborne C, Cryan PM, O'Shea TJ, Oko LM, Ndaluka C, Calisher CH, Berglund AD, Klavetter ML, Bowen RA, Holmes KV, Dominguez SR. 2011. Alphacoronaviruses in New World bats: prevalence, persistence, phylogeny, and potential for interaction with humans. PLoS One 6:e19156. https://doi.org/10.1371/journal.pone.0019156.

69. Macnaughton MR. 1982. Occurrence and frequency of coronavirus infections in humans as determined by enzyme-linked immunosorbent assay. Infect Immun 38:419–423. https://doi.org/10.1128/iai.38.2.419-423.1982.

70. Schmidt OW, Allan ID, Cooney MK, Foy HM, Fox JP. 1986. Rises in titers of antibody to human coronaviruses OC43 and 229E in Seattle families during 1975–1979. Am J Epidemiol 123:862–868. https://doi.org/10.1093/oxfordjournals.aje.a114315.

71. Griffin BD, Chan M, Tailor N, Mendoza EJ, Leung A, Warner BM, Duggan AT, Moffat E, He S, Garnett L, Tran KN, Banadyga L, Albietz A, Tierney K, Audet J, Bello A, Vendramelli R, Boese AS, Fernando L, Lindsay LR, Jardine CM, Wood H, Poliquin G, Strong JE, Drebot M, Safronetz D, Embury-Hyatt C, Kobasa D. 2021. SARS-CoV-2 infection and transmission in the North American deer mouse. Nat Commun 12:3612. https://doi.org/10.1038/s41467-021-23848-9.

72. Thompson JD, Higgins DG, Gibson TJ. 1994. CLUSTAL W: improving the sensitivity of progressive multiple sequence alignment through sequence weighting, position-specific gap penalties and weight matrix choice. Nucleic Acids Res 22:4673–4680. https://doi.org/10.1093/nar/22.22.4673.

73. Kumar S, Stecher G, Li M, Knyaz C, Tamura K. 2018. MEGA X: Molecular Evolutionary Genetics Analysis across computing platforms. Mol Biol Evol 35:1547–1549. https://doi.org/10.1093/molbev/msy096.